The concentration-discharge slope as a tool for water quality management

M.Z. Bieroza[1], A.L. Heathwaite[2], M. Bechmann[3], K. Kyllmar[1] and P. Jordan[4]

[1]Department of Soil and Environment, Swedish University of Agricultural Sciences, Uppsala, Box 7014, 750 07, Sweden, magdalena.bieroza@slu.se, katarina.kyllmar@slu.se

[2]Lancaster Environment Centre, Library Avenue, Lancaster University, Lancaster LA1 4YQ, United Kingdom, louise.heathwaite@lancaster.ac.uk

[3]Norwegian Institute of Bioeconomy Research, P.O. Box 115, NO-1431 Ås, Norway, marianne.bechmann@nibio.no

[4]School of Geography & Environmental Sciences, Ulster University, Coleraine, BT52 1SA, United Kingdom, p.jordan@ulster.ac.uk

Abstract

Recent technological breakthroughs of optical sensors and analysers have enabled matching the water quality measurement interval to the time scales of stream flow changes and led to an improved understanding of spatially and temporally heterogeneous sources and delivery pathways for many solutes and particulates. This new ability to match the chemograph with the hydrograph has promoted renewed interest in the concentration-discharge (*c*-*q*) relationship and its value in characterising catchment storage, time lags and legacy effects for both weathering products and anthropogenic pollutants. In this paper we evaluated the stream *c*-*q* relationships for a number of water quality determinands (phosphorus, suspended sediments, nitrogen) in intensively managed agricultural catchments based on both high-frequency (sub-hourly) and long-term low-frequency (fortnightly-monthly) routine monitoring data. We used resampled high-frequency data to test the uncertainty in water quality parameters (e.g. mean, 95th percentile and load) derived from low-frequency sub-datasets. We showed that the uncertainty in water quality parameters increases with reduced sampling frequency as a function of the *c*-*q* slope. We also showed that different sources and delivery pathways control *c*-*q*

relationship for different solutes and particulates. Secondly, we evaluated the variation in *c-q* slopes derived from the long-term low-frequency data for different determinands and catchments and showed strong chemostatic behaviour for phosphorus and nitrogen due to saturation and agricultural legacy effects. The *c-q* slope analysis can provide an effective tool to evaluate the current monitoring networks and the effectiveness of water management interventions. This research highlights how improved understanding of solute and particulate dynamics obtained with optical sensors and analysers can be used to understand patterns in long-term water quality time series, reduce the uncertainty in the monitoring data and to manage eutrophication in agricultural catchments.

Keywords

Eutrophication; Concentration-discharge relationship; Chemostatic behaviour; High-frequency monitoring; Long-term water quality time series; Phosphorus and Nitrogen

Highlights

- High-frequency data help to understand the patterns in long-term data
- Chemostatic responses lead to low errors in water quality parameters
- Low-order agricultural catchments homogenize stream solute responses
- Phosphorus and nitrogen chemostatic responses are driven by legacy stores
- Concentration-discharge slope helps to prioritise monitoring and mitigation efforts

Introduction

Combating eutrophication is proving difficult and exposes gaps in our scientific understanding of hydrological and biogeochemical processes controlling stream concentrations of solutes and particulates. The relative importance of these processes and contribution of dominant sources and delivery pathways is captured by the concentration-discharge (*c-q*) relationship. The *c-q* relationship characterises solute/particulate change (dilution or concentration) with varying flow (Evans and Davies, 1998) and can be quantified as the slope *b* of the *c-q* regression relationship on logarithmic axes (Godsey

et al., 2009). The *c*-*q* relationship is often complex due to hydrochemical variability but can generally be classified into two patterns: chemostatic ($|b|<0.1$) and chemodynamic ($|b|>0.1$) with either dilution ($b<-0.1$) or concentration ($b>0.1$) pattern. The chemostatic *c*-*q* pattern, in which the concentrations are stable over a large range of flows has been observed for many solutes and particulates with an abundant source of the chemical in the catchment (Thompson et al., 2011) e.g. weathering bedrock (Ameli et al., 2017; Godsey et al., 2009; Hoagland et al., 2017) or agricultural soils and the unsaturated zone (Basu et al., 2011; Van Meter et al., 2017). These sources are also referred to as the legacy stores that can control the mobilisation and stream transport of the chemicals in the long-term and lead to transport-limitation (Basu et al., 2011). When the rate of the concentration change is larger than the flow change, a chemodynamic *c*-*q* pattern and source-limitation are observed with either concentrations increasing (concentration) or decreasing (dilution). Recent increased availability of high-frequency (sub-hourly) *c* and *q* data, due to deployment of optical sensors and wet-chemistry analysers, has led to improved understanding of the complex *c*-*q* patterns observed in water quality data. For example, recent work explains how both seasonal and storm-to-storm dynamics in source mobilisation and activation of different delivery pathways control the chemostatic and chemodynamic *c*-*q* responses (Bieroza and Heathwaite, 2015; Lloyd et al., 2016).

To date, the *c*-*q* relationship has been evaluated for a large range of chemicals both derived from weathering of bedrock and from agricultural land use. The studies of *c*-*q* dynamics in agricultural catchments focus on chemicals that are of major concern due to increasing eutrophication and hypoxia of inland and coastal waters: phosphorus (P) both as total P (TP) and total and soluble reactive P (TRP and SRP) (Basu et al., 2011; Bieroza and Heathwaite, 2015; Dupas et al., 2015), suspended sediments (SS) measured directly or with turbidity (TURB) as a proxy (Lawler et al., 2006), organic and inorganic nitrogen (N), particularly in the form of nitrate-nitrogen (NO_3-N) (Bieroza et al., 2014; Dupas et al., 2016; Van Meter et al., 2017) and compounds that provide information on the general hydrochemical functioning of catchments: total and dissolved organic carbon (TOC and DOC) (Butturini et al., 2008; Hoagland et al., 2017) and specific conductivity (COND) (Bieroza and Heathwaite, 2015) .

Hydrochemical data have been collected for over 150 years (Howden et al., 2010) and most of these long-term datasets are from rivers (>4th Strahler order) and collected at low frequency (typically monthly) (Tetzlaff et al., 2017). Therefore, this existing water quality sampling method is not suited to target the highly variable, in space and time, agricultural P and N pollution in low-order (<3rd Strahler order) catchments (Bieroza et al., 2014). Recent advances in *in situ* water quality monitoring with optical sensors and wet-chemistry analysers (Bieroza and Heathwaite, 2016; Floury et al., 2017; Jordan et al., 2012; Rode et al., 2016) help to bridge this gap, but due to high-financial cost of the *in situ* technology per sampling site, new approaches that integrate the high- and low-frequency sampling are needed (Bieroza et al., 2014; Chappell et al., 2017; Jordan and Cassidy, 2011). To address this scientific and management need, we propose that the new knowledge of *c-q* dynamics obtained with high-frequency sampling can improve the understanding of hydrochemical patterns in readily available long-term datasets and can help to prioritise monitoring and mitigation efforts.

Specifically, we evaluated the uncertainty and variation in the *c-q* relationship for selected solutes and particulates, for a number of low-order small agricultural catchments in the UK, Norway and Sweden that are subjected to eutrophication pressures. We hypothesized that the *c-q* slope represents the catchment's tendency to store and transport chemicals and that it can be a useful tool in water management practice. Our objectives were to: **1)** evaluate the variation in the *c-q* slopes for P, SS, NO_3-N, DOC and COND for both high- and low-frequency sampling, **2)** evaluate the uncertainty in operational water quality parameters (mean, 95th percentile and load) derived from low-frequency datasets as a function of the *c-q* slope, **3)** provide recommendations on how the *c-q* slopes can help to improve water quality management.

Methods

High-frequency datasets

Two high-frequency datasets were used in the analysis: HF1 (Leith catchment, UK, 2009-2014, hourly and sub-hourly, TP, TRP, TURB, NO_3-N and COND) and HF2 (SE3 catchment, SE, 2017-2018, sub-hourly, TP, TRP, TURB, NO_3-N and DOC) with continuous flow discharge measurements. Similar

experimental setups were deployed in both cases, with stream water pumped to a small hut on the bank and the measurements conducted on unfiltered samples with wet-chemistry analysers (Systea's Micro Mac for HF1 and Hach Lange's Phosphax for HF2 giving TP and TRP) and in-line optical sensors for TURB and solutes (Systea's WaterWatch and Hach Lange's Nitratax for HF1 and s:can's Spectrolyser for HF2). The details of the HF1 experimental setup and principles of the *in situ* monitoring are given elsewhere (Bieroza and Heathwaite, 2015; Bieroza and Heathwaite, 2016; Bieroza et al., 2014). Both study catchments represent small, low-order catchments dominated by agricultural land use: grassland and livestock grazing in the Leith catchment (HF1 in Table 1) and arable land and crop production in the SE3 catchment (HF2 in Table 1). The catchments differ in terms of geology and soils, with sandstone and loam soils in HF1 and marine clay and heavy clay soils in HF2 with the effect on hydrology: intensive ground-surface water interactions (Krause et al., 2009) and subsurface flow pathways in HF1 (Bieroza et al., 2014) and overland, macropore and tile drainage flow pathways in HF2 (Ulén et al., 2011).

Low-frequency datasets

We collated long-term low-frequency water quality time series (TP, TRP and SRP, SS, NO_3-N, DOC and TOC and COND) for agricultural catchments subject to risk of eutrophication from three EU countries (UK, Norway and Sweden) spanning a range of climatic and soil conditions (USDA, 1987) (Table 1). The datasets varied in terms of sampling frequency: fortnightly sampling for the Swedish and Norwegian catchments under Agricultural Monitoring Programmes to 6-12 samples a year in the UK catchments under the routine monitoring programmes (Water Framework and Nitrates Directives).

In the UK, all environmental datasets were accessed online: the water quality datasets were obtained from the Environment Agency (http://environment.data.gov.uk/water-quality), flow records from the National River Flow Archive (https://nrfa.ceh.ac.uk/) and soil data from the UK Soil Observatory Map (http://www.ukso.org/home.html). As the UK does not have a specific agricultural impact monitoring programme, unlike Sweden and Norway, a selection of the sampling points and study catchments was made from over 1500 gauging stations and over 7000 water quality sampling points with the following

criteria: continuous (no breaks due to gauging station closure) flow discharge record, catchment area <60 km^2, agricultural land use >70%, no major settlements/fish farms/sewage treatment outlets in the catchment and a nearby water quality sampling point (up to 50 m upstream and 100 m downstream, with no tributaries between both points) with at least 50 TRP and NO_3-N measurements. Based on these criteria, a selection of 42 catchments representing diverse soil, climatic and agricultural conditions was made (Table 1). For the UK, DOC and TP measurements are not part of the routine monitoring (Table ST1).

In Norway, data about water quality and agricultural production are collected in the Agricultural Environmental Monitoring Programme (JOVA) (Bechmann et al., 2008). The selected ten catchments represent the main agricultural production systems in Norway including cereals (E), vegetables (S), intensive dairy farming (W) and more extensive grass production (S and N) and vary in terms of soils, topography and climate (Table 1). In all catchments, fortnightly flow-proportional samples are collected (TP, SRP, SS, NO_3-N) and water level is recorded automatically. Since the P, SS and NO_3-N concentrations and loads are high, economic subsidies and information campaigns have been introduced to reduce pollution trough e.g. reduction in autumn ploughing, improved nutrient and animal waste management and mitigation measures (buffer zones and constructed wetlands) (Bechmann et al., 2008).

In Sweden, ten small agricultural catchments (Table 1) have been monitored for agricultural impact on water quality for more than 20 years (Kyllmar et al., 2014). Fortnightly water quality sampling includes time-proportional grab sampling (1990-2010) and flow-proportional composite sampling (from 2005) for TP, TRP, SRP, NO_3-N, SS, DOC and COND with continuous flow discharge measurements. The catchments represent various types of soils, agricultural production and climate with a clear precipitation gradient between SW and E Sweden. Higher precipitation in the SW catchments results in higher flow discharge and nutrient loads (SE6, SE8 and SE9) compared to the E catchments (SE1, SE2, SE3 and SE5). As a result, the SW Sweden catchments have climatic and hydrological conditions similar to the UK and Norway (Table 1). Catchments with high clay content (SE9, SE10) generally have higher P and SS loads compared to those with sandy soils (SE8).

153 *Data analyses*

154 All high- and low-frequency datasets were quality controlled to remove outliers and calculate basic
155 descriptive statistics (Tables 2 and ST1). Flow discharge records were used to calculate the flashiness
156 index as a ratio of the high (5th percentile) and low flows (95th percentile) which describes the dominant
157 flow pathways in the catchment (Jordan et al., 2005). A higher flashiness index (Q5:Q95; Table 1)
158 indicates a higher ratio of flashier, faster flow responses to rainfall compared to slower, low flows
159 (baseflow and slow subsurface). For each high-frequency dataset, loads were calculated using a
160 standard algorithm based on instantaneous concentration and flow discharge (Bieroza et al., 2014;
161 Jordan and Cassidy, 2011) (Equation 1):

162 $$L = \frac{K\sum_{i=1}^{n} C_i Q_i}{\sum_{i=1}^{n} Q_i} Q_\Gamma \quad \text{(Equation 1)}$$

163 Where: C_i and Q_i are instantaneous high-frequency concentration and discharge data, L is the load
164 estimate, Q_Γ is the average flow discharge based on the long-term data, K is a constant which accounts
165 for the duration of the record, n is the number of concentration measurements.

166 To examine the effect of sampling frequency on the uncertainty in water quality parameters routinely
167 used for water management (mean, standard deviation, maximum and 95th percentile concentration,
168 load and *c*-*q* slope), the high-frequency datasets were resampled using 10,000 Monte Carlo iterations
169 each, to simulate daily, weekly, fortnightly and monthly sampling frequencies, respectively (Table 2).
170 For each simulated frequency (daily, weekly, fortnightly and monthly) 10,000 individual datasets were
171 created by randomly selecting samples from the high-frequency data with the single constraint criterion
172 – samples need to represent unique days, weeks, fortnights or months respectively. We calculated the
173 relative errors *e* for each water quality parameter and determinand (TP, TRP, TURB, NO_3-N, DOC and
174 COND) as Equation 2:

175 $$e = \frac{100(LF-HF)}{HF}\% \quad \text{(Equation 2)}$$

176 with an assumption that the high-frequency value *HF* (e.g. mean concentration or load) represents the
177 true value compared to the low-frequency value *LF* (Supplementary Tables ST2-7 and Supplementary

Figures SF1-3). The *c-q* slopes were calculated by fitting a linear regression to the log-transformed concentration and flow discharge data. To compare the differences in mean errors, concentrations and *c-q* slopes between the catchments and determinands, a non-parametric analysis of variance was used (Kruskal-Wallis test). To analyse the catchment controls (e.g. soil type and flashiness) on the *c-q* slopes and interactions between different determinands, a multivariate non-parametric canonical redundancy analysis (RDA) was performed (Bieroza and Heathwaite, 2015; Legendre and Legendre, 1998). Spearman's correlations *p*-values were corrected for multiple comparisons with a Bonferroni correction (Holm, 1978) and for all analyses a uniform significance level of 0.05 was used. All data processing and statistical analyses were carried out in MATLAB version 8.6 (R2015b).

Results

Concentration-discharge relationship for the high-frequency datasets

Comparison of the *c-q* relationships from the two high-frequency datasets (HF1 and HF2) showed that concentration effect ($b>0$) was predominant for both datasets with the exception of solutes: $NO_3\text{-}N_{HF1}$, $COND_{HF1}$ and TRP_{HF2}, all showing the dilution pattern ($b<0$; Figure 1). Three determinands ($NO_3\text{-}N_{HF1}$, $COND_{HF1}$ and TP_{HF2}) showed chemostatic behaviour ($|b|<0.1$) suggesting a predominant transport-limitation mechanism (Basu et al., 2011). TP_{HF1}, $TURB_{HF1}$ and $TURB_{HF2}$ showed chemodynamic behaviour ($|b|>0.1$) and source-limitation mechanism (b=0.36, 0.27 and 0.32). Two solutes ($NO_3\text{-}N_{HF2}$ and DOC_{HF2}) showed a step change from chemostatic (b=0.1 and 0.04) to chemodynamic behaviour (b=0.28 and 0.25) at q=0.01 m^3s^{-1} (Figure 1 and Table ST8). The *c-q* relationship for $COND_{HF1}$ showed non-linear curvature with two linear slopes fitted: b=-0.06 for flows 0-10 m^3s^{-1} and b=-0.26 for flows >10m^3s^{-1} (Table ST8).

The HF1 determinands (TP, TRP and TURB) showed a large scatter in the data due to seasonal and storm-to-storm variation in the *c-q* behaviour and hysteretic responses (Bieroza and Heathwaite, 2015). TP, TRP and TURB responded similarly in both study catchments, showing a concentration pattern. Conversely, $NO_3\text{-}N_{HF1}$ and $COND_{HF1}$ showed a weak dilution pattern, while $NO_3\text{-}N_{HF2}$ and DOC_{HF2} showed an overall concentration pattern in HF2. The TRP *c-q* pattern was the opposite to solutes in

both datasets – a concentration pattern in HF1 similar to TP and TURB and a dilution pattern in HF2 in contrast to both TP and TURB (Figure 1).

Uncertainty in water quality parameters estimated from the low-frequency datasets

To assess the uncertainty in derivation of water quality parameters from routine low-frequency monitoring, the high-frequency datasets were resampled to simulate daily, weekly, fortnightly and monthly sampling (Table 2). For all determinands, the mean and standard deviation of the resampled datasets were consistent with the values derived from the high-frequency datasets (suggesting that the errors were normally distributed), whereas the maximum gradually decreased with the sampling frequency (Table 2).

In general, the uncertainty increased for all parameters and determinands with decreasing sampling frequency (Tables ST2-7). The mean concentration, which is often used as an indicator of water quality status, was underestimated by the low-frequency sampling for TP and TURB. The errors in the mean TRP and NO_3-N concentrations showed two patterns: underestimation or both under- and over-estimation (Figures 2 and SF1-3). The lowest errors (<10%) were observed for $NO_3\text{-}N_{HF1}$ and $COND_{HF1}$ and the largest for TURB and TP with the greatest underestimations of -441% $TURB_{HF2}$, -305% $TURB_{HF1}$, -288% TP_{HF2} for the monthly datasets (Table ST2). Similar patterns were seen in the errors in calculation of the 95th percentile (Table ST5), instantaneous load (Table ST6) and the *c*-*q* slopes (Table ST7). The general trend was that determinands showing near-chemostatic *c*-*q* slopes ($NO_3\text{-}N_{HF1}$, $COND_{HF1}$, TP_{HF2} and TRP_{HF2}) had lower errors for all water quality parameters compared to the determinands with the chemodynamic slopes (Figures 2 and SF1-3). From all determinands, TURB showed the largest errors spanning three orders of magnitude for all low-frequency sampling simulations. This shows that only sub-hourly sampling can accurately capture the SS dynamics.

The observation that uncertainty in the water quality parameters derived from the low-frequency data is low for near-zero, chemostatic slopes ($|b|<0.1$) and high for chemodynamic *c*-*q* slopes ($|b|>0.1$) can be tested by plotting the mean *c*-*q* slope and mean parameter estimation error from 10,000 Monte Carlo simulations (Figure 3). The positive correlation (R^2=0.52) indicates that errors are small (0-20%) for

the low *c-q* slopes and increase with the increasing *c-q* slopes. Solutes showed lower slopes and errors and the highest values of slopes and errors were observed for both particulates and solutes. For the same determinand, the slopes can be different between catchments suggesting that distribution of the delivery pathways and catchment-specific processes play an important role in controlling the *c-q* relationship. The high variation in the load estimation errors for similar values of the *c-q* slopes for $TURB_{HF1}$, $TURB_{HF2}$ and TP_{HF2} can be seen in Figure 4. In contrast, $NO_3\text{-}N_{HF1}$ and $COND_{HF1}$ showed very little variation in the simulated *c-q* slopes and corresponding load estimation errors. The much wider range of the observed *c-q* slopes for the HF2 dataset can be explained by a more flashy catchment character compared to HF1 (Q5:Q95 237 to 74, Table 1). From all determinands, only the TRP_{HF2} showed a shift from a strong dilution pattern (*b*=-0.5) and high load overestimation (up to 50%) to near-chemostatic behaviour (*b*=-0.1) and small load estimation errors (10%, Figure 4).

Variation in the c-q relationship in the low-frequency datasets

To evaluate the variation in the *c-q* slopes for different determinands, we analysed available water quality time series for selected agricultural catchments in the UK, Norway and Sweden (Tables 1 and ST1). Mean concentrations (Table ST1) varied between determinands and countries (Figure 5). The Norwegian and Swedish catchments showed higher TP and SS and lower TRP and NO_3-N concentrations compared to the UK catchments. These differences result from different dominant geology and soil types: post-glacial clay geology and fine texture soils in the Norwegian and Swedish catchments (Kyllmar et al., 2014) with a high risk of TP and SS losses and permeable sediments with deep unsaturated zone in the UK catchments (Ascott et al., 2016) with a high risk of NO_3-N and TRP pollution (Bieroza et al., 2014).

Figure 6 shows the variation in the *c-q* slopes between determinands. TRP showed the largest variation with the *c-q* slopes from *b*=-0.6 (strong dilution pattern) to *b*=0.5 (strong concentration pattern). Two solutes, DOC and COND showed a typical chemostatic *c-q* behaviour with near-zero slope *b* values (-0.08 and 0.08 respectively) and a small variation in the *c-q* relationship. The SS concentrations showed a predominant concentration pattern (mean *b*=0.40) with slopes changing between -0.1 and 0.9, while

256 both TP and NO_3-N exhibited a weak chemostatic/concentration pattern (mean *b*=0.12 and 0.18
257 respectively). For the TP concentrations, the predominant type of the *c*-*q* relationship measured as a
258 single slope *b* will depend on the relative contribution of particulate and dissolved fractions of P. This
259 effect can be seen in Figure 1; for HF1 both the TP and TRP show similar *c*-*q* slopes as the TRP/TP
260 ratio is 85% but for HF2 (TRP/TP ratio is 60%) the TP slope is almost the arithmetic mean of the SS
261 (TURB) and TRP slopes. This averaging of the particulate and solute *c*-*q* behaviour for the TP results
262 in near-chemostatic behaviour for analysed agricultural catchments.

263 To evaluate the effect of catchment properties (Table 1) and mean determinand concentrations (Table
264 ST1) on the observed *c*-*q* slopes, we conducted a redundancy analysis (Figure 7). The catchment
265 properties explained 57% of the variance in the *c*-*q* slopes of TRP, SS and NO_3-N, with the b_{TRP}
266 positively correlated with the first canonical axis and b_{SS} negatively and $b_{NO3\text{-}N}$ positively correlated with
267 the second canonical axis. No significant effects of the catchment area, percentage of the agricultural
268 land use or Strahler order were observed since our study explicitly focuses on low order, small
269 agricultural catchments. The first canonical axis discriminated between catchments with high TRP
270 concentrations and a predominant dilution *c*-*q* pattern (e.g. UK24) and low TRP concentrations, high
271 rainfall and a predominant concentration *c*-*q* pattern (e.g. NO5). The second canonical axis
272 discriminated between flashy, clay catchments with low NO_3-N concentrations, chemostatic NO_3-N and
273 SS *c*-*q* response and well-drained, groundwater-dominated catchments with high positive *c*-*q* slopes for
274 SS and negative *c*-*q* slopes for NO_3-N (Figure 7). These results indicate that TRP and NO_3-N saturation
275 effects, catchment soil type and flashiness provide a good explanation of the observed differences in
276 the *c*-*q* slopes between the catchments and determinands.

277 *Robustness of the c-q relationship*

278 To test the robustness of the *c*-*q* relationship we compared the slopes for high- and low-frequency
279 datasets, different sampling strategies and nonlinear and non-stationary *c*-*q* relationships - in general
280 there were no significant differences. There were no statistically significant differences in the *c*-*q* slopes
281 calculated independently from the high- (HF1 and HF2) and low-frequency (LF1 and LF2) datasets

(Table ST1) despite much longer coverage of the low-frequency time series (HF1 2009-2015, LF1 1990-2015, HF2 2016-2017, LF2 1988-2016). There were no statistically significant differences between *c*-*q* slopes for different sampling strategies: time- and flow-proportional sampling for the Swedish catchments (Table ST1 and Figure SF4), despite both datasets only partially overlapping, e.g. for SE1 time-proportional (grab) 1992-2010 and flow-proportional 2004-2017. There was a strong linear relationship between the *c*-*q* slopes calculated from both datasets (R^2=0.88, p<0.05) and the data were generally grouped by the determinand (Figure SF4a) rather than the catchment (Figure SF4b).

We examined all datasets for the presence of nonlinear *c*-*q* relationships (as NO_3-N_{HF2} and DOC_{HF2} in Figure 1), visually determined the inflection point and fitted two separate linear slopes for low (≤ inflection point discharge) and high (≥ inflection point discharge) flows. Majority of the *c*-*q* relationships (92%) showed single linear slopes with the exception of the datasets listed in Table ST8 that showed changes in the *c*-*q* slope at a given threshold value of flow. The differences between single and dual slopes were significant for TP and SS but not for RP, NO_3-N, DOC or COND (Table ST8). The threshold value of flow discharge in nonlinear *c*-*q* relationships varied between determinands and catchments but in general low flows showed lower *c*-*q* slopes than high flows. Both TP and RP showed dilution pattern for low flows and strong concentration pattern for high flows, whereas SS slopes shifted from a moderate to strong concentration pattern (Figure 8). The single *c*-*q* slope reflected the dominant *c*-*q* relationship for TRP and SS and was the mean value of individual slopes for TP.

The *c*-*q* relationship can also be affected by non-stationarity in either *c* or *q* data e.g. due to the presence of a linear trend in the long-term time series. To test this effect, we calculated linear trends for all high- and low-frequency datasets (Table ST9) and expressed the slopes as an annual percentage trend (Figure 9). The mean annual trend varied from -2.2% for TRP to 0.4% for Q and TP and showed the largest variation between the catchments for SS (8.5% $SE2^{fp}$ and -17.9% $NO4^{fp}$), TRP (16.7% $SE7^{fp}$ and -16.8% UK5) and TP (10.5% $SE7^{fp}$ and -7.0% UK23). The high-frequency datasets showed higher annual trends (e.g. Q HF1 -9.7% and HF2 8.3%) likely due to a shorter length of the time series compared to the low-frequency, long-term datasets. To show the effect of significant linear trends with more than 5% annual change on the *c*-*q* slopes, the datasets were split in half and the *c*-*q* slopes were

calculated independently for each half (Figure SF5). There were no statistically significant differences between the *c-q* slopes for TP, TRP and SS but the effect varied between the datasets and determinands (Figure SF5). An example (Figure SF6) shows two time series with similar annual trends (-8.4% and -7.8%) TRP (UK6) and NO_3-N ($NO4^{fp}$), however the slopes were different only for TRP as indicated by the dilution pattern (*b*=-0.16) in the first half and minor concentration pattern (*b*=0.09) in the second half of the time series. For NO_3-N in the catchment NO4, similar slopes were observed potentially due to NO_3-N saturation and consistent chemostatic response over time.

Discussion

c-q slope variation between determinands and catchments

Recent studies highlight that catchment size and dominant land use can be predictors of the variation in concentrations (Abbott et al., 2018; Musolff et al., 2015) and the *c-q* relationship (Moatar et al., 2017). They show that the variation in the concentrations and nutrient retention declines with the catchment area for both solutes and particulates (Abbott et al., 2018; Cheng and Basu, 2017) and can lead to universal homogenization of the hydrochemical responses downstream in the river network (Basu et al., 2011; Creed et al., 2015). Adding to this homogenization, are the legacy stores of P and N in agricultural soils and unsaturated zone controlling water quality in the long-term for both small (Ascott et al., 2016; Bieroza et al., 2014; Dupas et al., 2016) and large catchments (Howden et al., 2010; Van Meter et al., 2017). A recent study (Bieroza and Heathwaite, 2015) showed that a low-order agricultural stream is a position in the stream network where both the hydrological and biogeochemical processes operate jointly to control the *c-q* relationship leading to a dynamic equilibrium between the chemostatic and chemodynamic responses.

This ongoing research, focusing on large (catchment size and land use) or small scale (storm flow and meteorological controls) controls of the *c-q* relationship, suggest that headwater catchments (<3rd Strahler order) are critical landscape positions where most of the stream flow and hydrochemical signature of the stream network is generated. These headwater catchments are also the basic landscape units of water quality management and critical areas for combating eutrophication and hypoxia through

agri-environmental mitigation measures (Ockenden et al., 2017). Our study adds new evidence to this ongoing work by analysing the variability in the *c-q* relationships for a range of determinands and small, low-order agricultural catchments.

Our results (Figure 6) indicate homogenization of the *c-q* responses in intensively managed agricultural catchments with many determinands showing typical chemostatic behaviour – a small range of concentrations compared to flow variation. This indicates that despite a large catchment-to-catchment variation in the *c-q* relationship, the net effect of agricultural management in headwater catchments on stream chemistry is chemostatic. This averaging potentially results from two reasons. Firstly, solutes (DOC, COND and NO_3-N) surprisingly show a very narrow range of *c-q* slopes for catchments that vary significantly in terms of bedrock, soil type, climate and hydrology. A tendency towards chemostatic *c-q* relationship in the intensively managed catchments can be a result of agricultural land use overriding the structural differences between catchments (soil, vegetation and topography) and homogenization of hydrological responses (Basu et al., 2011). The long-term agricultural land use leads to shortening of the flow pathways and residence time that will in turn affect many hydrological and biogeochemical processes. Secondly, a large variation in the *c-q* slopes including both positive and negative values observed between the catchments and determinands can lead to apparent averaging of the *c-q* responses downstream the river network. This synchrony at the catchment level has been show recently by Abbott et al. (2018) for two nested agricultural catchments. Our results confirm similar effects for a large number of catchments with agricultural land use, varying in geology, climate and soils. On the determinand level, the averaging effect can be exemplified by the *c-q* responses of RP (dilution pattern) and SS (concentration pattern). These opposing effects result in the near-chemostatic responses for the TP, when the contribution of particulate and soluble fractions of P is similar. Also, some determinands and catchments show dual slopes for low and high flows with the opposing effect on the *c-q* slopes e.g. dilution at low flows and concentration at high flows for TRP, leading to an overall chemostatic *c-q* effect.

The general strong affinity towards certain *c-q* behaviour, also shown by Moatar et al. (2017) in the >50 km^2 catchments, was not observed for TRP and NO_3-N *c-q* responses. For the catchments analysed in

362 our study, subjected to diffuse pollution with no major point sources, with high concentrations the
363 typical response is dilution for TRP and chemostasis for NO_3-N, whereas a concentration pattern is
364 observed for the catchments with lower concentrations (Figure 7). This links to the presence of the P
365 and N legacy stores in agricultural catchments due to excess fertilisation over a long time. The effect of
366 P and N saturation in agricultural catchments on the *c-q* relationship depends on the geology, soil type
367 and the flashiness. In permeable catchments with deep unsaturated zone and low flashiness, excess
368 NO_3-N will gradually accumulate in the subsurface (Ascott et al., 2016; Howden et al., 2010; Van Meter
369 et al., 2017) and produce a chemostatic *c-q* response in the stream (Bieroza et al., 2014). In poorly-
370 drained clay catchments, due to shorter residence times in the subsurface excess NO_3-N will be flushed
371 on a storm-to-storm basis leading to a concentration *c-q* response in the stream, as in HF2. The TRP
372 behaviour is more complex due to its transport duality – it can be transported both as a solute along the
373 subsurface flow pathways (Mellander et al., 2015) and sorbed to particulates and transported along the
374 surface flow pathways (Dupas et al., 2015). A concentration *c-q* pattern is typical for P derived from
375 diffuse agricultural sources but the presence of small rural point sources leads to a dilution pattern at
376 low flows (Withers et al., 2012). When both types of P sources are present, the *c-q* relationship is
377 nonlinear (Figure 8). The transient TRP storage (in bed sediments (Jarvie et al., 2005) or in the riparian
378 zone (Dupas et al., 2015) can also lead to nonlinear *c-q* relationship by introducing delays in stream
379 delivery and hysteretic *c-q* relationships (Bieroza and Heathwaite, 2015; Hoagland et al., 2017).

380 A growing body of research suggests that the *c-q* slope expresses the relative importance between
381 hydrological and biogeochemical controls (Basu et al., 2011; Thompson et al., 2011). Recent analysis
382 of storm events showed that the chemostatic *c-q* responses indicated the dominance of hydrological
383 controls and the chemodynamic *c-q* responses indicated the dominance of biogeochemical controls
384 (Bieroza and Heathwaite, 2015). The *c-q* slope encapsulates both the individual effects of
385 biogeochemical and hydrological process and their synergistic effects and thus represents the
386 catchment's tendency to store and transport solutes and particulates. However, these processes are non-
387 stationary and future land management and climate change will modify their relative balance (Basu et
388 al., 2011). This combined effect on water quality can be difficult to predict due to positive and negative

feedbacks between the effect of land management and climate change (Ockenden et al., 2017). We suggest that the *c-q* slope can be a good measure of catchment's response and resilience to future change. Future land management is likely to reduce P and N concentrations in agricultural catchments, alleviate the effects of P and N saturation and thus reduce the legacy effects on water quality while increased rainfall can increase the flashiness of the catchments, also due to higher seasonal gradients in flow conditions (Ockenden et al., 2017). Our results (Figure 7) suggest that this potential future change scenario (lower NO_3-N and TRP concentrations, higher rainfall and flashiness) will shift the *c-q* responses in agricultural catchments from chemostatic to chemodynamic (concentration). Apart from being an indicator of these changes, higher *c-q* slopes will also mean a more dynamic *c-q* relationship and a higher uncertainty in water quality parameters.

Errors in water quality parameters as a function of the c-q slopes

Previous work focused on the advantages and limitations of the high-frequency *in situ* monitoring in comparison with the traditional low-frequency grab sampling (Bieroza et al., 2014; Cassidy and Jordan, 2011; Dupas et al., 2016; Floury et al., 2017). These studies showed how the gain in number of observations due to high-frequency monitoring leads to improved load estimation compared to both actual and re-sampled low-frequency time series, specifically for the flashy catchments and P and SS concentrations (Cassidy and Jordan, 2011; Jordan and Cassidy, 2011; Rozemeijer et al., 2010). The load estimation errors were also compared for determinands showing different stream transport mechanisms – the chemodynamic *c-q* responses for P and chemostatic for NO_3-N (Bieroza et al., 2014). The authors concluded that the chemostatic *c-q* pattern resulted in much lower load estimation errors compared to chemodynamic pattern for P and was driven by the groundwater legacy store of NO_3-N. Here, we build on this work and show the errors not only for loads but also for other parameters used in water quality management: *c-q* slope, mean concentration used as an indicator of the water quality status e.g. for P in the Water Framework Directive (Wade et al., 2012), the 95^{th} percentile used to select water bodies at a risk of pollution e.g. to designate Nitrate Vulnerable Zones.

Similarly to previous studies, we showed that errors increase with decreasing sampling frequency, are higher for particulates than solutes and are higher for determinands exhibiting chemodynamic *c-q* behaviour, specifically the concentration pattern. The range of errors observed in our study corresponded well with previous studies (Bieroza et al., 2014; Cassidy and Jordan, 2011), however by not constraining the sampling to typical sampling regimes (e.g. from 9 to 5), we were able to estimate the maximum possible errors. One of the main findings was that underestimation of parameters derived from low-frequency sampling was more severe than overestimation. Most determinands and parameters showed a maximum of one order of magnitude overestimations while the underestimations could reach three orders of magnitude. This could be a serious limitation of the low-frequency sampling for determinands showing highly dynamic flow responses e.g. SS and for flashy catchments with clay soils. For these determinands and catchments, there is a critical need to conduct high-frequency water quality measurements, particularly if those locations are also at high risk of failing to achieve good ecological status. Another limitation could be the estimation of the 95th percentile from the low-frequency NO_3-N sampling for the catchments showing chemodynamic *c-q* responses e.g. HF2. In this case the potential underestimation of the 95th percentile is up to two orders of magnitude (Table ST5) and could lead to not designating the catchment as a Nitrate Vulnerable Zone.

The errors in the *c-q* slopes followed the same pattern as for the other parameters, low errors for chemostatic and high errors for chemodynamic *c-q* slopes. However, the *c-q* slope errors reduced the strength of the effect (e.g. from strong concentration to weak concentration effect) rather than completely changed it (e.g. from the concentration to dilution). The uncertainty in the *c-q* slopes was also reduced for longer time series. This means that for most of the available long-term water quality time series, the *c-q* slope should adequately capture the catchment's dominant behaviour in storing and transporting chemicals. The *c-q* pattern for a given determinand persists even if the sampling changes (e.g. from time- to flow-proportional) or the concentrations show a linear trend. Both cases should however always be checked for potential errors due to differences between flow-proportional and grab sample concentrations or averaging concentration and dilution patterns over time or for different flows in time series exhibiting temporal trends.

As our results show, the simple correlation between *c-q* slope and potential parameter estimation error (Figure 3) should be analysed with caution. Determinands delivered from a number of different sources or during different periods can exhibit different *c-q* patterns, therefore a good understanding of the main delivery pathways and times when they are active is needed to understand when the errors are likely to be high. Also, for the same determinand and the value of the *c-q* slope the errors can be enhanced by catchment properties (Figure 3 $TURB_{HF2}$) e.g. by the presence of fast delivery pathways as in the tile drained clay catchments. For example, NO_3-N showed highly chemostatic behaviour for HF1 likely due to nitrate saturation in the unsaturated zone but a step change from chemostatic to chemodynamic behaviour for HF2. For the clay catchment HF2, due to higher erosion risk, the load estimation errors for TURB were much higher compared with the similar *c-q* slope for HF1. In special cases, when it is evident from the visual inspection of the data that two different *c-q* relationships exist for different flows, fitting separate linear regressions is needed. However, for many headwater catchments, the long-term low-frequency datasets have too few samples to calculate statistically significant *c-q* slopes for different flows, in contrast to high order streams and rivers (Moatar et al., 2017) where 2/3 of cases showed dual slopes (in our study less than 8%). We found that single slopes capture well the dominant *c-q* relationship for cases where samples were collected at all flows. If there is a bias in the sampling e.g. towards low flows, measurements at high flows are needed to adequately represent the *c-q* relationship, dominant sources and delivery pathways. This can be achieved either by targeting storms with conventional sampling or by deploying *in situ* optical sensors (Bieroza et al., 2014).

c-q slope as a robust water quality management tool

Our study shows that the *c-q* slope is a robust descriptor of the catchment's tendency to store and transport chemicals, since similar slopes were observed for both HF and LF datasets and different sampling strategies (time- vs flow-proportional). It can provide a rapid indication of the catchment's status and resilience towards a given chemical – if the chemical exhibits the chemostatic or negative *c-q* slopes the catchment is likely to be saturated with that chemical, whereas if the chemical shows the concentration pattern its delivery is likely to be transport-limited. In the latter case, appropriate mitigation measures to intercept dominant delivery pathways and target critical source areas could help

to reduce pollution. In the case of chemostatic solute behaviour, individual measures and short-term solutions can be ineffective, as is often the case for the catchments failing to meet good water quality status (Harris and Heathwaite, 2012). For these catchments, both long-term and large-scale mitigation approaches are needed (Ockenden et al., 2017; Van Meter et al., 2017) that will require a good cooperation between decision makers, farmers and scientists.

Many water quality monitoring programmes are facing financial cuts that will inevitably result in the reduction of the sampling network. Water managers are therefore faced with critical questions: which sampling locations to keep, which long-term time series to continue and how to optimise the sampling to the local conditions. The *c-q* slope could help address many of these challenges. The optimal sampling frequency required to capture the full range of particulate and solute behaviour depends on their *c-q* slopes. For chemicals with a chemostatic *c-q* pattern (e.g. NO_3-N and COND), low-frequency sampling (weekly to monthly) for all flows is sufficient to capture the *c-q* dynamics and obtain accurate estimates of water quality parameters. For chemicals with a dilution *c-q* pattern (e.g. TRP), daily to weekly sampling is needed to adequately characterise low flow concentrations and target diffuse sources at high flows. Finally, for chemicals with a concentration *c-q* pattern (e.g. TURB and SS but also TP and NO_3-N), it is critical to target individual storm events at hourly time step as there is a large variation in the concentrations depending on distribution of the sources and hydrological connectivity. When selecting the sampling locations which should be retained, a priority should be given to those with a large variation in the *c-q* responses between determinands as indicative of the heterogeneous sources and delivery pathways, with dual slopes and chemodynamic patterns. The latter locations are more likely to be pivot points to the water quality in the stream network as they can experience large variations in concentrations (up to three orders of magnitude) over short storm flows (Bieroza et al., 2014). Dual *c-q* slope relationships (e.g. dilution at low flows and concentration at high flows) indicate that different sampling regimes and different mitigation measures need to be considered for different combinations of source and delivery pathways. For any water quality monitoring network, the individual sampling points can be optimised depending on their dominant *c-q* patterns, in terms of sampling frequency and flow conditions to be targeted.

Changes in the *c-q* slope can also aid the location and subsequent evaluation of land management interventions e.g. in the form of mitigation measures to reduce agricultural losses of P, SS and N. To achieve the best environmental outcomes, the mitigation measures should be placed to intercept the main sources and delivery pathways. This spatial targeting can be achieved with critical source areas and critical pathways mapping (Abbott et al., 2018; Thomas et al., 2016) but also by evaluating the *c-q* slopes as discussed above. Improvements in water quality in catchments with a dilution-concentration P pattern are likely to be more difficult to achieve compared to uniform *c-q* patterns, and will require targeting both low flow (septic tanks or riparian zone) and high flow (diffuse catchment or in-stream) sources. The evaluation of the effectiveness of these mitigation measures can be achieved using *c-q* slopes both in time (by comparing low and high flows or periods before and after implementation of the measures) and space (by comparing locations upstream and downstream of the measures). This critical evidence obtained with *c-q* slopes is needed both for water managers to comply with the statutory requirements and the farming community to see that their efforts in building and maintaining mitigation measures bring the desired environmental benefits.

Conclusions

The *c-q* slope is a single metric that expresses the catchment's dominant tendency for storing and transporting solutes and particulates, is easy to calculate from readily available hydrochemical datasets and can be used to effectively guide water quality management. The *c-q* slope can be used to understand solute and particulate behaviour across spatial (from stream reaches to stream networks and between catchments) and temporal scales, and by this to extrapolate beyond single catchment process understanding (Abbott et al., 2016). As it encapsulates information about dominant biogeochemical and hydrological controls, the *c-q* slope is a good measure of current balance and future change in any of the underlying processes, e.g. due to land management including mitigation measures or climate change. Agricultural catchments analysed in our study had no major point sources and showed on average strong chemostatic behaviour for TP and NO_3-N due to long-term accumulation of agricultural N and P in unsaturated zone and soils. Future reduction in P and N pollution, increased rainfall and

flashiness in agricultural catchments are likely to shift this dominant chemostatic behaviour to chemodynamic, concentration *c-q* responses to flow. For water managers, this shift will require a more targeted approach to water quality monitoring, both in space and time, since the chemodynamic *c-q* slopes have higher uncertainty in the diagnostic parameters derived from low-frequency sampling e.g. loads, mean or 95th percentile concentrations. To achieve the best outcomes, water management should focus on catchments and determinands showing chemodynamic and dual slope *c-q* responses. The *c-q* slope analysis combined with high-frequency monitoring using optical sensors and analysers can provide an effective toolset to evaluate the effectiveness of management interventions. By focusing on low-order agricultural catchments, we provide a critical understanding of the linkages between hydrochemical functioning and eutrophication risks and translate this knowledge into operational responses.

Acknowledgements

This work was funded by the Marie Skłodowska-Curie Fellowship awarded to M. Bieroza (Project HotPaNTS, 657192, European Commission). The authors would like to also acknowledge the funding from the Natural Environment Research Council (NE/M019837/1 awarded to M. Bieroza and NE/G001707/1 awarded to A.L. Heathwaite) and from the Stiftelsen Lantbruksforskning awarded to M. Bieroza (O-16-23-640). The authors would like to thank Lars Bergström from the Swedish University of Agricultural Sciences, Alwyn Hart and Linda Pope from the Environmental Agency, Neil Mullinger and Paddy Keenan from the Lancaster Environment Centre, Maria Blomberg and Lovisa Sternman-Forsberg from the Swedish Monitoring Programme and Mattias Ryman and Niklas Strömbeck from Luode Co.

References

Abbott BW, Baranov V, Mendoza-Lera C, Nikolakopoulou M, Harjung A, Kolbe T, et al. Using multi-tracer inference to move beyond single-catchment ecohydrology. Earth-Science Reviews 2016; 160: 19-42.

Abbott BW, Gruau G, Zarnetske JP, Moatar F, Barbe L, Thomas Z, et al. Unexpected spatial stability of water chemistry in headwater stream networks. Ecol Lett 2018; 21: 296-308.

548 Ameli AA, Beven K, Erlandsson M, Creed IF, McDonnell JJ, Bishop K. Primary weathering rates,
549 water transit times, and concentration-discharge relations: A theoretical analysis for the critical
550 zone. Water Resources Research 2017.
551 Ascott MJ, Wang L, Stuart ME, Ward RS, Hart A. Quantification of nitrate storage in the vadose
552 (unsaturated) zone: a missing component of terrestrial N budgets. Hydrological Processes 2016;
553 30: 1903-1915.
554 Basu NB, Thompson SE, Rao PSC. Hydrologic and biogeochemical functioning of intensively managed
555 catchments: A synthesis of top-down analyses. Water Resources Research 2011; 47: 1-12.
556 Bechmann M, Deelstra J, Stålnacke P, Eggestad HO, Øygarden L, Pengerud A. Monitoring catchment
557 scale agricultural pollution in Norway: policy instruments, implementation of mitigation
558 methods and trends in nutrient and sediment losses. Environmental Science & Policy 2008; 11:
559 102-114.
560 Bieroza MZ, Heathwaite AL. Seasonal variation in phosphorus concentration–discharge hysteresis
561 inferred from high-frequency in situ monitoring. Journal of Hydrology 2015; 524: 333-347.
562 Bieroza MZ, Heathwaite AL. Unravelling organic matter and nutrient biogeochemistry in groundwater-
563 fed rivers under baseflow conditions: Uncertainty in in situ high-frequency analysis. Sci Total
564 Environ 2016; 572: 1520-1533.
565 Bieroza MZ, Heathwaite AL, Mullinger NJ, Keenan PO. Understanding nutrient biogeochemistry in
566 agricultural catchments: the challenge of appropriate monitoring frequencies. Environ Sci
567 Process Impacts 2014; 16: 1676-91.
568 Butturini A, Alvarez M, Bernal S, Vazquez E, Sabater F. Diversity and temporal sequences of forms of
569 DOC and NO3-discharge responses in an intermittent stream: Predictable or random
570 succession? Journal of Geophysical Research 2008; 113.
571 Cassidy R, Jordan P. Limitations of instantaneous water quality sampling in surface-water catchments:
572 Comparison with near-continuous phosphorus time-series data. Journal of Hydrology 2011;
573 405: 182-193.
574 Chappell NA, Jones TD, Tych W. Sampling frequency for water quality variables in streams: Systems
575 analysis to quantify minimum monitoring rates. Water Res 2017; 123: 49-57.
576 Cheng FY, Basu NB. Biogeochemical hotspots: Role of small water bodies in landscape nutrient
577 processing. Water Resources Research 2017.
578 Creed IF, McKnight DM, Pellerin BA, Green MB, Bergamaschi BA, Aiken GR, et al. The river as a
579 chemostat: fresh perspectives on dissolved organic matter flowing down the river continuum.
580 Canadian Journal of Fisheries and Aquatic Sciences 2015; 72: 1272-1285.
581 Dupas R, Gascuel-Odoux C, Gilliet N, Grimaldi C, Gruau G. Distinct export dynamics for dissolved
582 and particulate phosphorus reveal independent transport mechanisms in an arable headwater
583 catchment. Hydrological Processes 2015; 29: 3162-3178.
584 Dupas R, Jomaa S, Musolff A, Borchardt D, Rode M. Disentangling the influence of hydroclimatic
585 patterns and agricultural management on river nitrate dynamics from sub-hourly to decadal
586 time scales. Sci Total Environ 2016; 571: 791-800.
587 Evans C, Davies TD. Causes of concentration/discharge hysteresis and its potential as a tool for analysis
588 of episode hydrochemistry. Water Resources Research 1998; 34: 129-137.
589 Floury P, Gaillardet J, Gayer E, Bouchez J, Tallec G, Ansart P, et al. The potamochemical symphony:
590 new progress in the high-frequency acquisition of stream chemical data. Hydrology and Earth
591 System Sciences 2017; 21: 6153-6165.
592 Godsey SE, Kirchner JW, Clow DW. Concentration-discharge relationships reflect chemostatic
593 characteristics of US catchments. Hydrological Processes 2009; 23: 1844-1864.
594 Harris GP, Heathwaite AL. Why is achieving good ecological outcomes in rivers so difficult?
595 Freshwater Biology 2012; 57: 91-107.
596 Hoagland B, Russo TA, Gu X, Hill L, Kaye J, Forsythe B, et al. Hyporheic zone influences on
597 concentration-discharge relationships in a headwater sandstone stream. Water Resources
598 Research 2017.
599 Holm S. A Simple Sequentially Rejective Multiple Test Procedure. Scandinavian Journal of Statistics
600 1978; 6: 65-70.

Howden NJK, Burt TP, Worrall F, Whelan MJ, Bieroza M. Nitrate concentrations and fluxes in the River Thames over 140 years (1868-2008): are increases irreversible? Hydrological Processes 2010; 24: 2657-2662.
Jarvie HP, Jürgens MD, Williams RJ, Neal C, Davies JJL, Barrett C, et al. Role of river bed sediments as sources and sinks of phosphorus across two major eutrophic UK river basins: the Hampshire Avon and Herefordshire Wye. Journal of Hydrology 2005; 304: 51-74.
Jordan P, Cassidy R. Technical Note: Assessing a 24/7 solution for monitoring water quality loads in small river catchments. Hydrology and Earth System Sciences 2011; 15: 3093-3100.
Jordan P, Melland AR, Mellander PE, Shortle G, Wall D. The seasonality of phosphorus transfers from land to water: implications for trophic impacts and policy evaluation. Sci Total Environ 2012; 434: 101-9.
Jordan P, Menary W, Daly K, Kiely G, Morgan G, Byrne P, et al. Patterns and processes of phosphorus transfer from Irish grassland soils to rivers—integration of laboratory and catchment studies. Journal of Hydrology 2005; 304: 20-34.
Krause S, Heathwaite L, Binley A, Keenan P. Nitrate concentration changes at the groundwater-surface water interface of a small Cumbrian river. Hydrological Processes 2009; 23: 2195-2211.
Kyllmar K, Forsberg LS, Andersson S, Mårtensson K. Small agricultural monitoring catchments in Sweden representing environmental impact. Agriculture, Ecosystems & Environment 2014; 198: 25-35.
Lawler DM, Petts GE, Foster ID, Harper S. Turbidity dynamics during spring storm events in an urban headwater river system: the Upper Tame, West Midlands, UK. Sci Total Environ 2006; 360: 109-26.
Legendre L, Legendre P. Numerical Ecology. Amsterdam: Elsevier Scientific Pub. Co., 1998.
Lloyd CE, Freer JE, Johnes PJ, Collins AL. Using hysteresis analysis of high-resolution water quality monitoring data, including uncertainty, to infer controls on nutrient and sediment transfer in catchments. Sci Total Environ 2016; 543: 388-404.
Mellander P-E, Jordan P, Shore M, Melland AR, Shortle G. Flow paths and phosphorus transfer pathways in two agricultural streams with contrasting flow controls. Hydrological Processes 2015; 29: 3504-3518.
Moatar F, Abbott BW, Minaudo C, Curie F, Pinay G. Elemental properties, hydrology, and biology interact to shape concentration-discharge curves for carbon, nutrients, sediment, and major ions. Water Resources Research 2017.
Musolff A, Schmidt C, Selle B, Fleckenstein JH. Catchment controls on solute export. Advances in Water Resources 2015; 86: 133-146.
Ockenden MC, Hollaway MJ, Beven KJ, Collins AL, Evans R, Falloon PD, et al. Major agricultural changes required to mitigate phosphorus losses under climate change. Nat Commun 2017; 8: 161.
Rode M, Wade AJ, Cohen MJ, Hensley RT, Bowes MJ, Kirchner JW, et al. Sensors in the Stream: The High-Frequency Wave of the Present. Environ Sci Technol 2016; 50: 10297-10307.
Rozemeijer JC, van der Velde Y, van Geer FC, de Rooij GH, Torfs PJJF, Broers HP. Improving Load Estimates for NO3and P in Surface Waters by Characterizing the Concentration Response to Rainfall Events. Environmental Science & Technology 2010; 44: 6305-6312.
Tetzlaff D, Carey SK, McNamara JP, Laudon H, Soulsby C. The essential value of long-term experimental data for hydrology and water management. Water Resources Research 2017; 53: 2598-2604.
Thomas IA, Mellander PE, Murphy PNC, Fenton O, Shine O, Djodjic F, et al. A sub-field scale critical source area index for legacy phosphorus management using high resolution data. Agriculture, Ecosystems & Environment 2016; 233: 238-252.
Thompson SE, Basu NB, Lascurain J, Aubeneau A, Rao PSC. Relative dominance of hydrologic versus biogeochemical factors on solute export across impact gradients. Water Resources Research 2011; 47: n/a-n/a.
Ulén B, Djodjic F, Etana A, Johansson G, Lindström J. The need for an improved risk index for phosphorus losses to water from tile-drained agricultural land. Journal of Hydrology 2011; 400: 234-243.

655 USDA. Module 3 - USDA Textural Soil Classification. Study Guide. United States Department of
656 Agriculture, Soil Mechanics Level I 1987: 1-53.
657 Wade AJ, Palmer-Felgate EJ, Halliday SJ, Skeffington RA, Loewenthal M, Jarvie HP, et al.
658 Hydrochemical processes in lowland rivers: insights from in situ, high-resolution monitoring.
659 Hydrology and Earth System Sciences 2012; 16: 4323-4342.
660 Van Meter KJ, Basu NB, Van Cappellen P. Two centuries of nitrogen dynamics: Legacy sources and
661 sinks in the Mississippi and Susquehanna River Basins. Global Biogeochemical Cycles 2017;
662 31: 2-23.
663 Withers PJA, May L, Jarvie HP, Jordan P, Doody D, Foy RH, et al. Nutrient emissions to water from
664 septic tank systems in rural catchments: Uncertainties and implications for policy.
665 Environmental Science & Policy 2012; 24: 71-82.

666

Table 1 Study catchment characteristics including permeability (high H, moderate M and low L), soil texture, Strahler order, mean rainfall and runoff flashiness (Jordan et al., 2005). Agricultural land use comprises arable, horticulture and grassland land uses. Soil texture: clay (C), clay loam (CL), silt loam (SiL), loam (L), sandy loam (SaL), sand (Sa), silt (Si), loamy sand (LSa), silty clay (SiC) (USDA, 1987). UK soil data were obtained from the UK Soil Observatory Map Viewer (http://www.ukso.org/home.html), and flow data from the National River Flow Archive (https://nrfa.ceh.ac.uk/). Catchment codes: HF – high-frequency dataset, LF – low-frequency dataset, SE1-10 Swedish catchments, NO1-10 Norwegian catchments and UK1-42 UK catchments. Water quality monitoring starting year is also given

Catchment	Area (km^2)	Longitude, latitude	Perm e-ability	Soil texture	Agricultural land use (%)	Strahler order	Rainfall (mm)	Flashiness (Q5:Q95)	Water quality monitoring from
HF1 (LF1)	54.0	-2.6, 54.5	M	CL, SiL	85	3	957^	74	2009/1990
HF2 (LF2)	7.4	16.1, 58.3	L	C	54	2	594*	237	2017/1988
SE1	33.0	17.1, 59.6	M	CL	59	2	623*	605	1992
SE2	16.3	14.9, 58.5	H	SaL	89	2	506*	279	1988
SE3	7.4	16.1, 58.3	L	C	54	2	594*	237	1988
SE4	1.8	13.4, 57.2	H	LSa	70	2	1066*	103	1993
SE5	4.7	18.5, 57.7	H	SaL	84	2	587*	372	1989
SE6	7.8	12.9, 56.2	M	C, SaL	86	2	719*	330	1988
SE7	8.3	13.2, 55.4	H	SaL, L	93	2	709*	556	1992
SE8	13.9	13.3, 56.7	M	SaL, SiL	85	2	886*	17	1996
SE9	7.6	12.7, 58.4	L	C	92	2	655*	214	1988
SE10	5.7	16.1, 59.2	L	C	56	2	539*	605	1993
NO1	4.5	10.8, 59.6	H	LSa	61	2	785[x]	38	1993
NO2	6.8	11.3, 60.1	L	SiC	65	3	665	42	1990
NO3	3.1	10.7, 60.8	L	C	68	2	585[x]	17	1985
NO4	1.7	10.7, 59.3	L	CL	62	1	829[x]	10	2004
NO5	0.9	8.4, 58.3	H	Sa	48	2	1230[x]	8	1991
NO6	19.4	8.7, 60.6	L	SiC	80	3	892[x]	79	1992
NO7	29.3	5.7, 59.9	L	C	85	2	1180[x]	20	1995
NO8	1.0	5.6, 58.7	H	LSa	88	1	1180[x]	7	1985
NO9	1.5	14.7, 67.2	H	Sa	35	2	1020[x]	19	1994
NO10	1.7	9.0, 61.1	H	LSa	41	1	575[x]	11	1991
UK1	9.0	-0.3, 55.2	M	CL	86	2	669*	80	2000
UK2	57.2	-0.3, 54.0	H	L	95	3	699*	12	2000
UK3	41.9	-0.7, 53.8	H	SaL	87	2	690*	14	2000
UK4	47.0	-0.9, 53.9	L	CL	86	3	654*	39	2000
UK5	12.9	-0.6, 54.2	M	L	90	2	735*	15	2000
UK6	32.2	-1.2, 53.2	H	SaL	77	2	668*	4	2000
UK7	46.2	-0.1, 53.1	L	CL	86	3	655*	8	2000
UK8	55.2	0.0, 53.4	H	SaL	90	2	699*	9	2000
UK9	54.7	-0.4, 53.4	M	CL	96	3	614*	46	2000
UK10	48.4	-0.4, 53.0	M	L	87	2	601*	168	2000
UK11	50.5	-0.6, 52.9	H	SaL	88	3	656*	12	2000
UK12	51.3	-0.6, 52.8	H	SaL	83	3	642*	41	2010
UK13	20.8	-0.9, 52.5	L	C	90	3	648*	127	2000
UK14	22.3	-0.5, 52.7	M	CL	71	3	616*	19	2000
UK15	58.3	-0.7, 52.4	M	CL	74	3	634*	18	2000
UK16	38.8	-0.6, 51.9	M	SaL	91	4	640*	53	2006
UK17	59.0	0.5, 52.9	H	Sa	90	2	688*	9	2000
UK18	28.3	1.0, 52.5	H	L	89	2	608*	26	2000
UK19	36.4	0.3, 52.2	H	SiL	90	2	565*	7	2000
UK20	47.7	0.5, 52.8	H	Sa	87	2	685*	5	2000

UK21	16.0	0.0, 52.1	H	SiL	70	2	561*	6	2000
UK22	59.8	1.5, 52.8	H	SiL	88	3	589*	65	2007
UK23	49.3	1.4, 52.2	M	SaL	81	2	631*	3	2000
UK24	54.9	0.9, 52.0	M	L	88	3	597*	16	2010
UK25	53.9	0.7, 52.1	M	SiL	90	2	566*	10	2000
UK26	47.4	0.7, 52.0	H	SaL	91	3	589*	30	2000
UK27	58.6	0.5, 52.0	H	SaL	95	3	560*	38	2000
UK28	28.3	0.6, 51.8	H	L	94	3	589*	215	2000
UK29	60.7	0.0, 51.7	L	CL	83	2	572*	6	2000
UK30	38.4	0.2, 51.8	L	C	72	2	616*	88	2000
UK31	54.6	0.2, 51.9	L	CL	83	3	599*	44	2000
UK32	25.9	0.0, 51.9	M	SaL	73	2	609*	24	2013
UK33	50.4	-1.3, 51.4	H	Sa	93	3	625*	36	2000
UK34	49.2	-1.7, 51.4	H	SaL	84	1	716*	8	2000
UK35	59.2	-1.9, 51.7	H	SaL	86	1	769*	129	2000
UK36	18.5	1.3, 51.3	H	SaL	77	2	702*	48	2000
UK37	37.7	-2.1, 51.6	H	SaL	87	1	723*	73	2000
UK38	28.2	-2.3, 52.6	M	CL	89	2	792*	53	2000
UK39	54.9	-2.5, 52.8	M	L	78	3	706*	17	2000
UK40	25.0	-2.2, 52.3	H	Sa	92	2	677*	8	2000
UK41	53.4	-2.4, 52.8	M	SaL	81	2	653*	12	2000
UK42	33.6	-0.4, 51.8	M	SaL	93	3	712*	13	2000

*1961-1990, ^1999–2014, ˣ1990-2015

Table 2 Resampled water quality datasets (mean number of samples ***N***, mean concentration ***μ***, standard deviation of the concentration ***δ*** and maximum value ***Max***) based on 10,000 Monte Carlo iterations

Parameter	**Sampling**	**HF1**				**HF2**			
		N	***μ***	***δ***	***Max***	***N***	***μ***	***δ***	***Max***
TP (mgl^{-1})	*HF*	18 364	0.04	0.08	1.63	7 024	0.28	0.12	1.40
	Daily	764	0.04	0.08	0.99	144	0.27	0.11	0.88
	Weekly	110	0.04	0.07	0.60	22	0.28	0.10	0.50
	Fortnightly	55	0.04	0.07	0.42	11	0.28	0.09	0.42
	Monthly	26	0.04	0.06	0.28	6	0.27	0.08	0.34
TRP (mgl^{-1})	*HF*	32 688	0.04	0.03	0.99	7 024	0.16	0.06	0.34
	Daily	997	0.03	0.03	0.43	144	0.16	0.06	0.33
	Weekly	143	0.03	0.03	0.22	22	0.16	0.06	0.27
	Fortnightly	71	0.03	0.03	0.17	11	0.16	0.06	0.25
	Monthly	33	0.03	0.03	0.13	6	0.15	0.06	0.20
TURB (NTU)	*HF*	44 893	2.48	4.61	242.20	13 766	35.12	39.70	838.72
	Daily	1 209	2.36	4.89	94.30	185	34.75	38.14	314.57
	Weekly	175	2.40	4.53	46.92	27	36.78	34.88	154.09
	Fortnightly	87	2.38	4.19	33.15	14	35.65	32.37	113.07
	Monthly	42	2.37	3.67	21.58	7	34.88	28.96	78.55
NO_3-N (mgl^{-1})	*HF*	36 779	2.33	0.47	7.46	13 763	3.14	3.27	11.91
	Daily	799	2.45	0.47	4.60	185	3.14	3.27	10.20
	Weekly	115	2.46	0.47	3.75	27	3.29	3.07	9.87
	Fortnightly	58	2.46	0.47	3.56	14	3.19	3.04	9.39
	Monthly	27	2.46	0.46	3.38	7	3.12	2.93	6.99
COND/DOC	*HF*	42 890	425.03	69.50	1291.00	13 766	27.61	11.09	71.78
($\mu Sm^{-1}/mgl^{-1}$)	*Daily*	1 158	434.59	64.62	1042.65	185	27.53	11.06	61.72
	Weekly	167	434.54	63.92	702.34	27	28.20	11.29	52.05
	Fortnightly	83	434.68	63.22	623.59	14	27.46	11.09	47.71
	Monthly	40	435.30	61.75	565.75	7	27.49	11.40	42.99

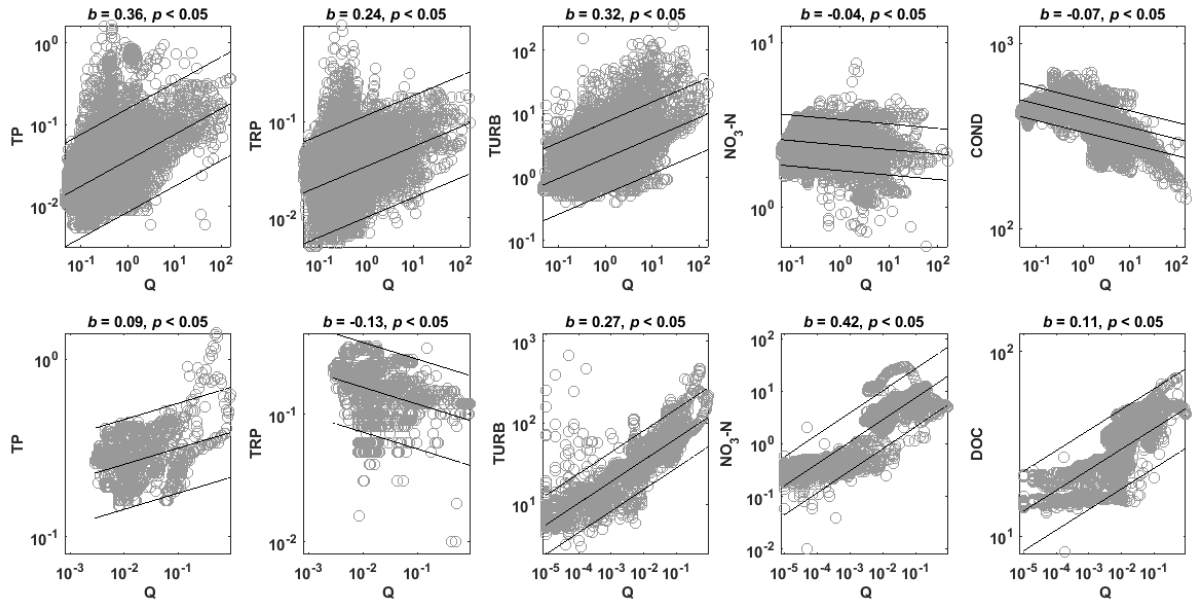

Figure 1 Concentration-discharge (*c*-*q*) relationship for the two high-frequency datasets (**HF1** top row and **HF2** bottom row) including the following determinands TP, TRP, TURB, NO_3-N and COND/DOC (columns). Slope of the *c*-*q* relationship *b* is given along with the *p* value. Both axes are in logarithmic scale

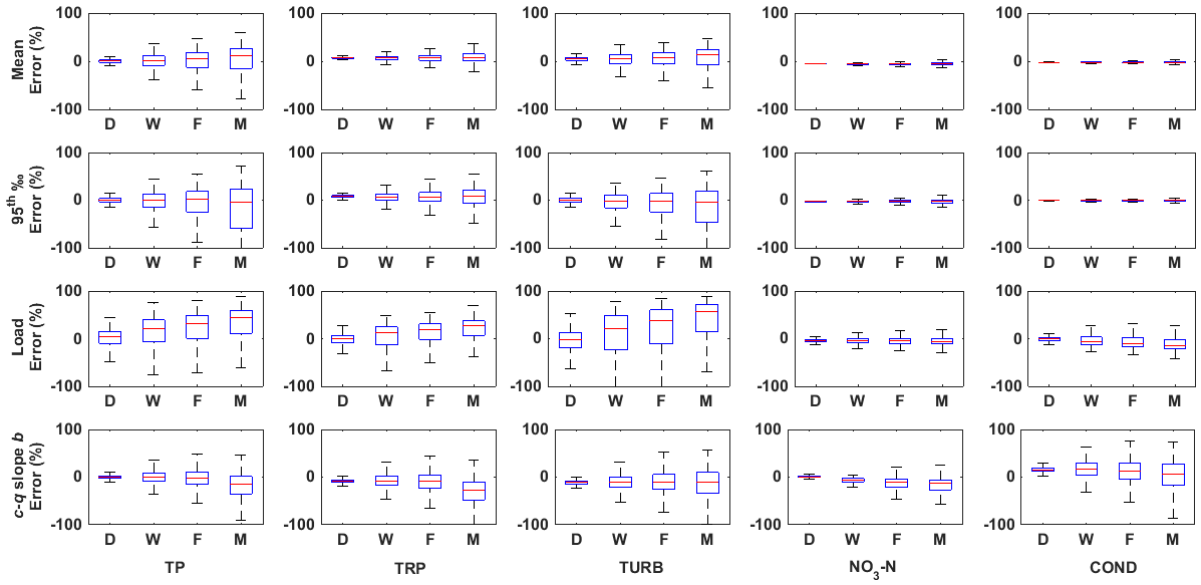

Figure 2 Relative errors in mean (top row), 95th percentile (second row), load estimation (third row) and *c*-*q* slope (bottom row) for **HF1** for TP, TRP, TURB, NO_3-N and COND. The central red mark is the median, the edges of the box are the 25th and 75th percentiles, the black whiskers extend to the most extreme data points. For better clarity the figure does not contain outliers (given in Supplementary Figure SF1)

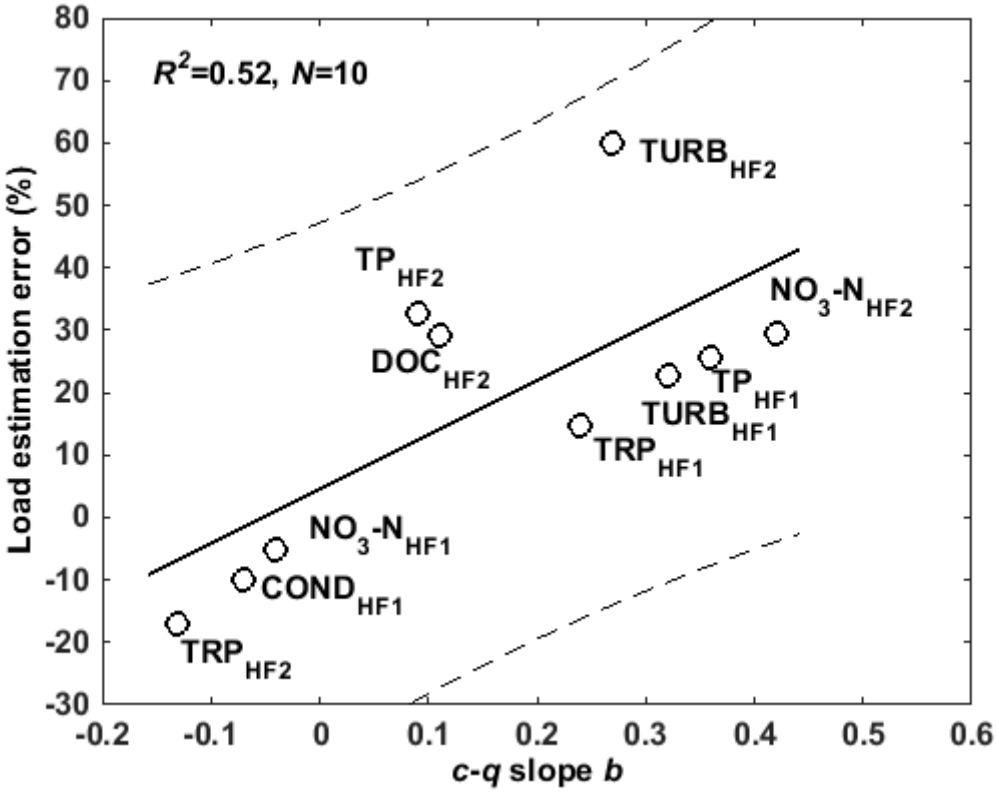

Figure 3 Relationship between *c-q* slope *b* and mean relative error in load estimation based on the 10,000 Monte Carlo simulation for all determinands in HF1 and HF2

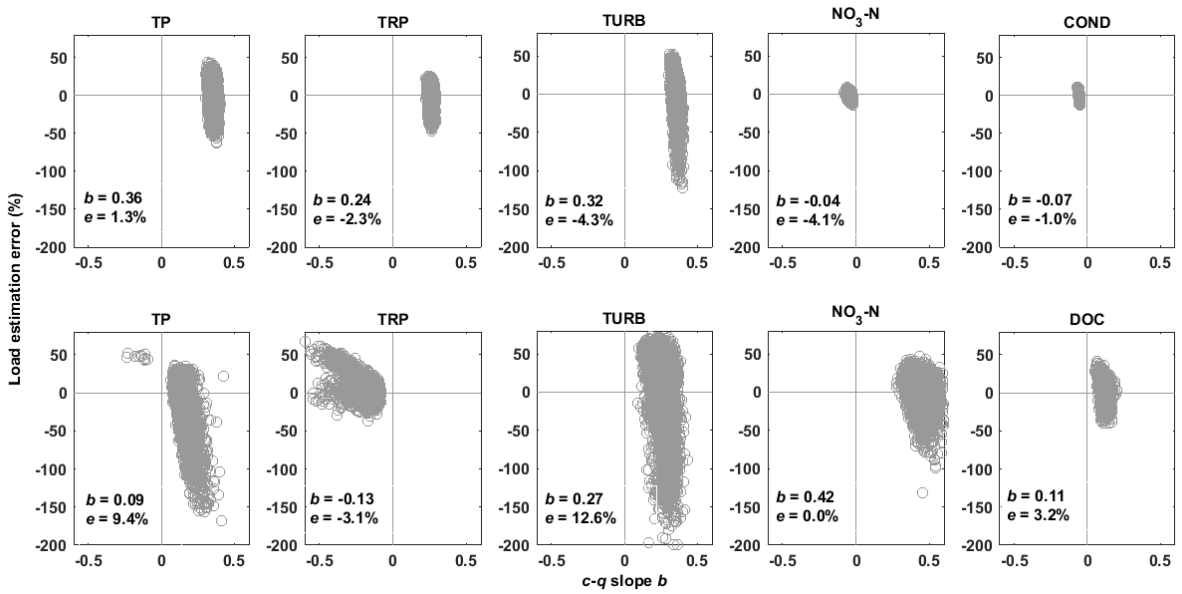

Figure 4 Daily load estimation errors (%) vs. *c*-*q* slope *b* based on 10,000 Monte Carlo simulations for two high-frequency datasets (HF1 top row and HF2 bottom row). Mean slope *b* and load estimation error *e* are given

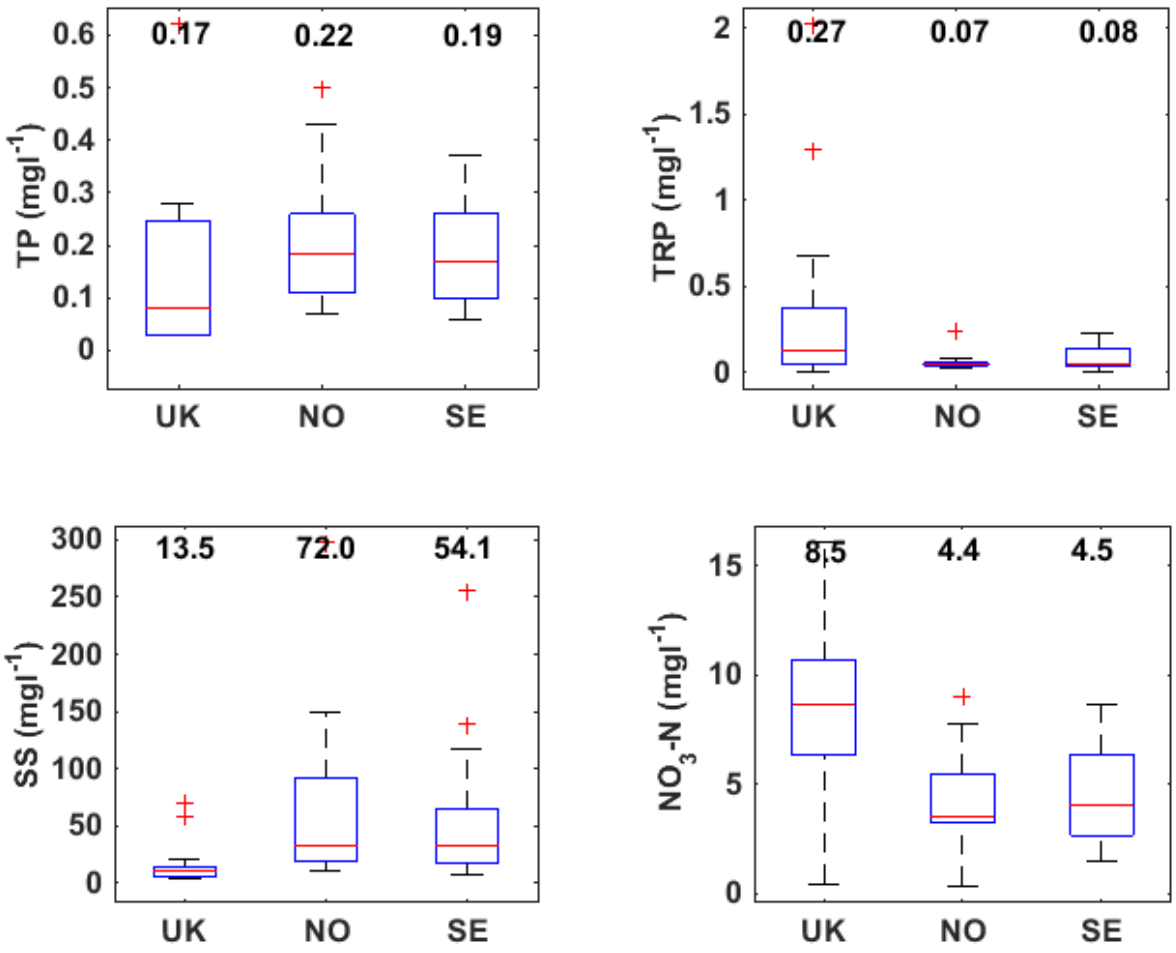

Figure 5 Analysis of variance (Kruskal-Wallis one-way ANOVA) for the mean TP, TRP, SS and NO_3-N concentrations per catchments' location (UK, Norway NO and Sweden SE). The central red mark is the median, the edges of the box are the 25th and 75th percentiles, the black whiskers extend to the most extreme data points and outliers are plotted as red crosses. Mean values are given as numbers

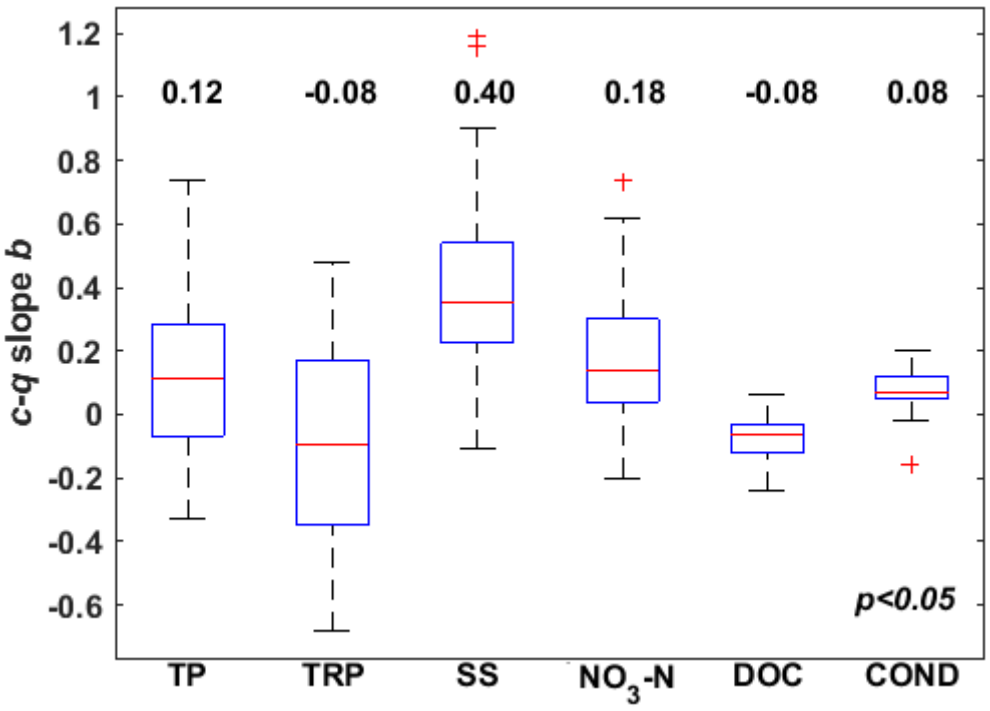

Figure 6 Analysis of variance (Kruskal-Wallis one-way ANOVA) for the *c-q* slopes per determinand (*N*=76). The central red mark is the median, the edges of the box are the 25th and 75th percentiles, the black whiskers extend to the most extreme data points and outliers are plotted as red crosses. Mean values are given as numbers above boxplots

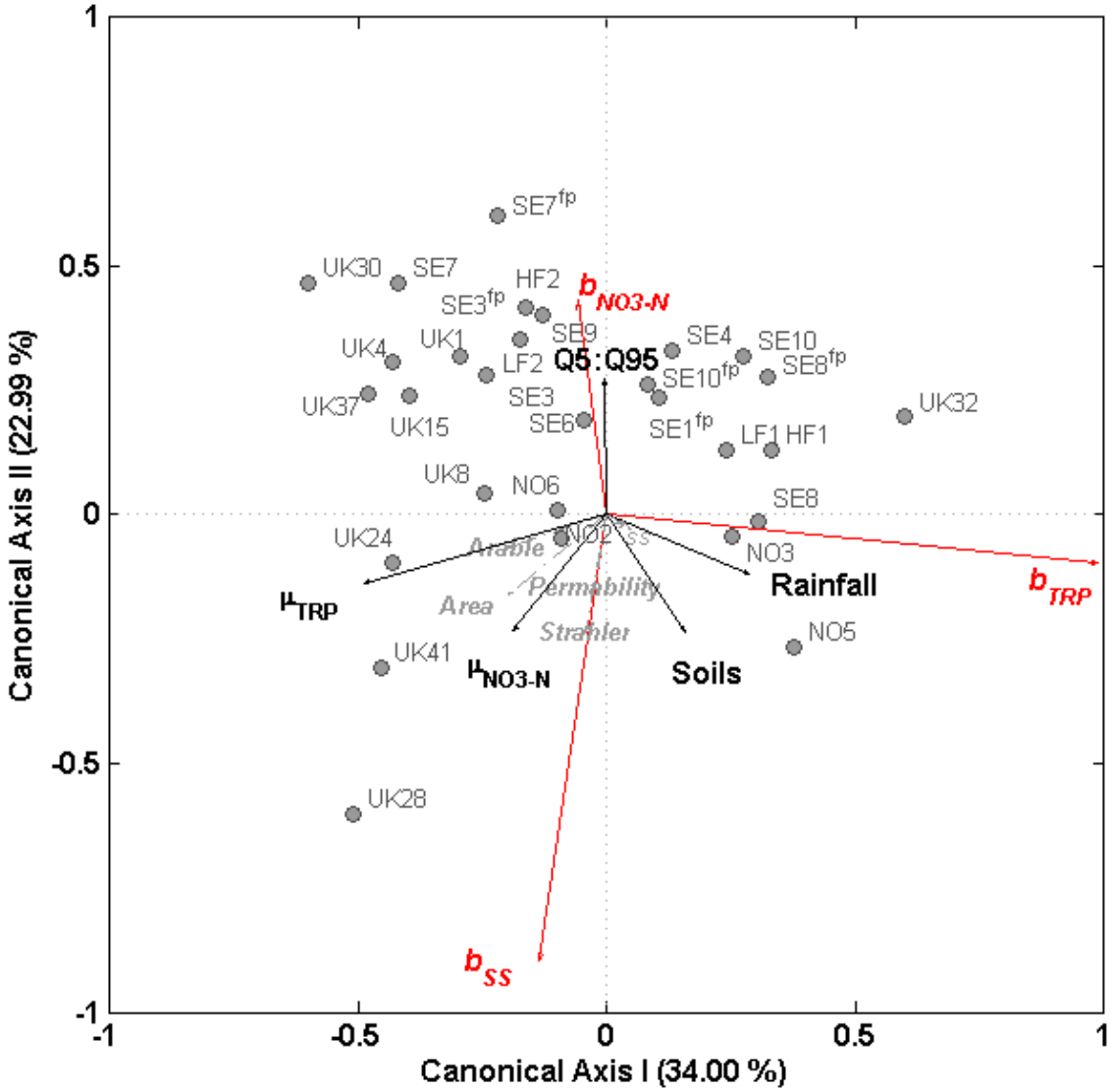

Figure 7 The redundancy analysis distance biplot showing ordination of selected explanatory (Area – catchment area, Arable – agricultural land use percentage, Permeability – 1 low, 2 moderate and 3 high, Q5:Q95 - the flashiness index, Soils - soil texture 1 clay soils, 2 loam soils and 3 sand soils, Strahler order; Table 1) and response variables (*c*-*q* slopes b_{TRP}, b_{SS} and $b_{NO3\text{-}N}$). The length of explanatory vectors indicates strength of the relationship with the scores of canonical axes. Distances among individual catchments (grey dots) are approximations of their Euclidean distances. Projecting a catchment at the right angle onto the response vector approximates a value of the *c*-*q* slope for that determinand. The angles between response and explanatory vectors indicate their correlation (Legendre and Legendre, 1998)

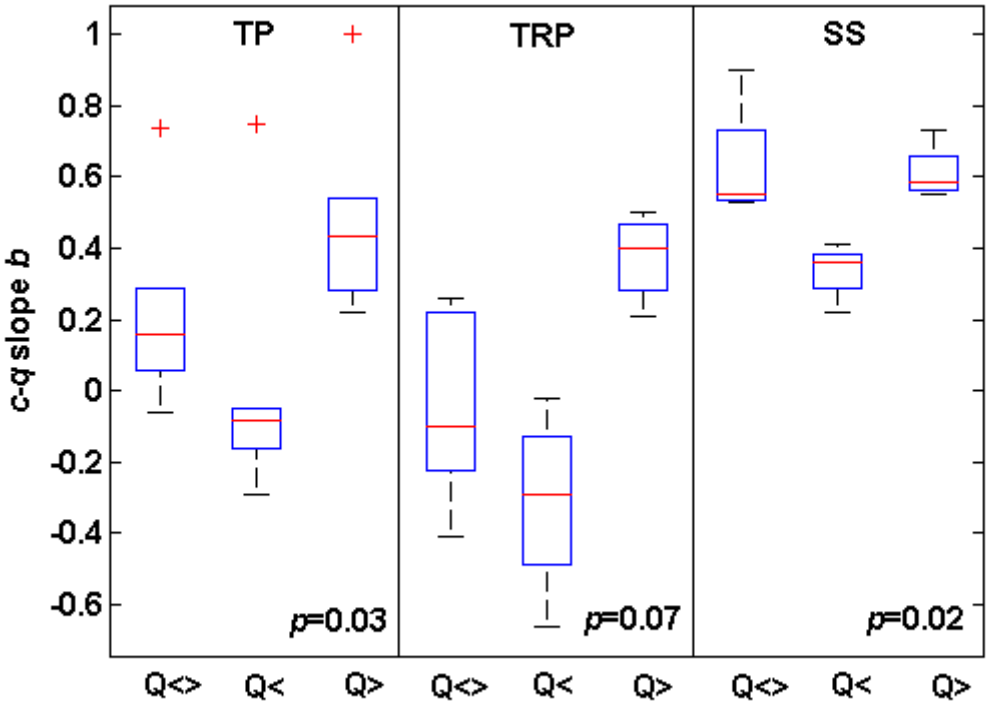

Figure 8 Analysis of variance (Kruskal-Wallis one-way ANOVA) for the *c-q* relationships showing step changes (*N*=6) in slope values: single linear slope (**Q<>**) and two linear *c-q* slopes (**Q<** for flows lower than the threshold value Q and **Q>** for flows higher than the threshold value Q). The data are also shown in Supplementary Table ST8. The central red mark is the median, the edges of the box are the 25th and 75th percentiles, the black whiskers extend to the most extreme data points and outliers are plotted as red crosses

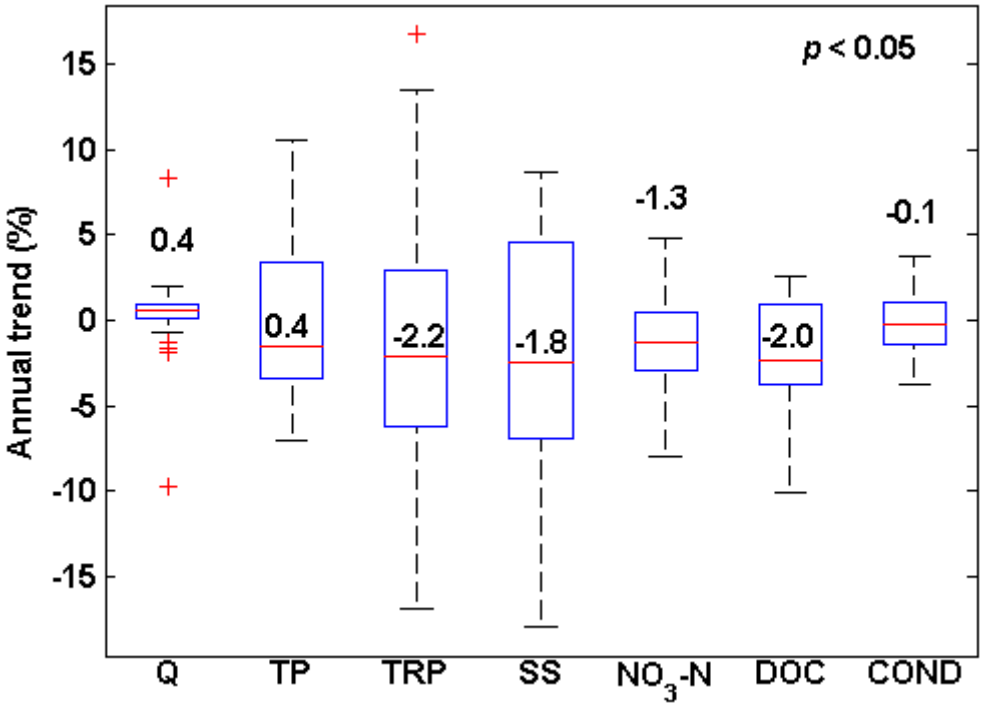

Figure 9 Analysis of variance (Kruskal-Wallis one-way ANOVA) for the annual linear trends per determinand for the flow and water quality datasets (*N*=76). The data are also shown in Supplementary Table ST9. The central red mark is the median, the edges of the box are the 25th and 75th percentiles, the black whiskers extend to the most extreme data points and outliers are plotted as red crosses. Mean values are given as numbers

Legendre L, Legendre P. Numerical Ecology. Amsterdam: Elsevier Scientific Pub. Co., 1998.

Supplementary Table ST1 Water chemistry in the study catchments: ***N*** number of measurements, ***μ*** mean, ***δ*** standard deviation and *c-q* slopes ***b***. Slopes which are not significant at 0.05 level are marked with ~~strikethrough~~. Flow-proportional sampling results are marked with [fp]

	TP (mgl^{-1})				**RP** (mgl^{-1})				**SS** (mgl^{-1})				**NO_3-N** (mgl^{-1})				**DOC/COND** ($mgl^{-1}/\mu Sm^{-1}$)			
	N	***μ***	***δ***	***b***	***N***	***μ***	***δ***	***b***	***N***	***μ***	***δ***	***b***	***N***	***μ***	***δ***	***b***	***N***	***μ***	***δ***	***b***
HF1	18.3k	0.04	0.08	0.36	32.6k	0.04	0.03	0.24	44.9k	2.48	4.61	0.32	36.8k	2.33	0.47	-0.04	42.9k	425.0	69.5	-0.07
LF1	314	0.07	0.08	0.29	565	0.06	0.14	0.17	435	6.3	12.5	0.35	561	2.96	1.10	0.01	91	551.1	70.5	-0.05
HF2	7024	0.28	0.12	0.09	7024	0.16	0.06	-0.13	13.8k	35.12	39.7	0.27	13.8k	3.14	3.27	0.42	13.8k	27.61	11.09	0.11
LF2	905	0.28	0.18	-0.09	903	0.16	0.13	-0.22	877	69.80	87.40	0.36	898	2.82	2.55	0.30	605	13.33	5.72	0.06
SE1	544	0.10	0.09	0.11	537	0.04	0.03	~~-0.01~~	518	44.18	80.96	0.44	553	1.58	1.23	0.32	520	9.87	4.61	0.05
SE2	698	0.08	0.10	-0.07	519	0.04	0.07	~~0.00~~	562	10.20	21.42	0.09	676	6.01	4.48	0.62	541	13.53	14.38	-0.16
SE3	905	0.28	0.18	-0.09	903	0.16	0.13	-0.22	877	69.80	87.40	0.36	898	2.82	2.55	0.30	605	13.33	5.72	0.06
SE4	569	0.09	0.06	~~0.00~~	526	0.02	0.01	0.03	539	12.23	9.43	0.07	570	3.31	1.07	-0.13	569	18.55	7.87	0.15
SE5	570	0.11	0.17	0.03	324	0.07	0.16	~~0.05~~	523	8.38	15.88	0.04	559	4.87	5.03	0.74	514	8.67	5.19	~~0.00~~
SE6	693	0.16	0.14	0.06	461	0.06	0.04	-0.07	649	34.92	63.01	0.34	694	6.38	2.88	0.08	549	9.78	5.17	0.07
SE7	705	0.37	0.54	-0.33	547	0.23	0.38	-0.43	611	14.72	31.31	0.04	702	8.64	3.01	0.03	579	12.61	7.90	0.01
SE8	490	0.06	0.07	0.42	448	0.01	0.02	0.25	471	17.56	30.64	0.53	493	8.15	1.83	0.06	493	7.90	2.65	0.20
SE9	994	0.23	0.22	-0.05	923	0.12	0.12	-0.16	911	37.71	102.5	0.34	992	3.39	2.68	0.44	324	9.33	6.05	~~0.04~~
SE10	596	0.20	0.21	0.30	303	0.05	0.05	0.21	593	53.27	105.6	0.29	596	1.54	1.43	0.34	592	11.89	6.42	0.11
SE1[fp]	296	0.16	0.10	0.15	289	0.04	0.02	0.06	284	93.53	97.03	0.32	297	1.81	1.08	0.17	295	10.01	4.28	0.05
SE2 [fp]	320	0.07	0.08	-0.07	317	0.03	0.05	~~0.02~~	298	17.60	18.80	-0.09	320	5.89	3.29	0.31	319	15.84	3.47	~~0.09~~
SE3 [fp]	212	0.34	0.16	-0.09	212	0.16	0.12	-0.19	211	117.5	100.9	0.15	209	2.95	2.07	0.19	211	13.14	4.87	~~0.02~~
SE4 [fp]	297	0.14	0.16	-0.06	297	0.03	0.02	~~0.02~~	294	28.32	48.48	-0.10	297	2.52	0.67	-0.08	297	20.42	8.69	0.05
SE5 [fp]	256	0.25	0.27	-0.15	256	0.17	0.18	-0.15	250	21.29	29.26	~~-0.06~~	254	6.42	5.48	0.40	255	7.93	5.77	~~0.00~~
SE6 [fp]	306	0.18	0.15	0.08	304	0.06	0.03	~~0.01~~	301	59.62	52.62	0.30	305	4.74	1.47	0.04	305	8.71	3.56	0.09
SE7 [fp]	253	0.27	0.25	-0.25	253	0.15	0.15	-0.28	243	31.19	59.84	-0.11	253	6.81	2.37	0.07	253	10.44	3.10	-0.02
SE8 [fp]	311	0.10	0.08	0.12	310	0.02	0.01	0.22	310	31.06	25.91	0.19	312	7.13	1.25	0.04	312	7.85	2.65	0.16
SE9 [fp]	290	0.33	0.27	0.19	287	0.08	0.05	~~0.01~~	280	255.0	334.7	0.41	289	2.90	3.01	0.18	286	10.05	7.04	0.19
SE10 [fp]	184	0.22	0.15	0.17	183	0.05	0.02	0.05	182	138.8	178.4	0.34	184	1.69	1.50	0.27	184	11.60	4.68	0.11
NO1[fp]	491	0.21	0.19	0.33	490	0.04	0.06	0.17	492	91.23	164.6	0.59	-	-	-	-	-	-	-	-

NO2 fp	395	0.50	0.49	0.27	396	0.06	0.06	-0.09	396	297.4	413.4	0.54	396	3.46	1.90	-0.08	-	-	-	-
NO3 fp	661	0.08	0.13	0.37	654	0.03	0.03	0.21	661	21.00	53.54	0.56	661	7.80	3.53	0.04	-	-	-	-
NO4 fp	111	0.43	0.39	-0.13	111	0.24	0.23	-0.22	111	46.32	81.56	-0.03	111	9.03	4.73	0.01	-	-	-	-
NO5 fp	450	0.26	0.34	0.74	421	0.05	0.03	0.37	450	52.26	92.91	0.89	448	4.17	2.24	0.23	-	-	-	-
NO6 fp	586	0.26	0.27	0.21	204	0.08	0.09	-0.09	583	149.4	260.6	0.54	586	3.48	2.25	0.05	-	-	-	-
NO7 fp	542	0.15	0.11	-0.02	207	0.05	0.05	0.12	335	11.18	9.95	0.17	536	3.52	1.17	0.15	-	-	-	-
NO8 fp	432	0.16	0.14	0.05	432	0.06	0.05	0.15	432	11.39	17.39	0.00	429	4.75	1.11	-0.07	-	-	-	-
NO9 fp	576	0.11	0.09	0.15	576	0.06	0.06	0.14	576	19.53	25.07	0.53	576	0.38	0.28	-0.03	-	-	-	-
NO10 fp	501	0.07	0.15	0.26	501	0.03	0.10	0.02	498	20.57	46.21	0.38	501	2.58	1.13	0.12	-	-	-	-
UK1	-	-	-	-	139	0.17	0.11	-0.26	96	12.03	15.51	0.36	141	3.01	2.00	0.38	65	888.9	460.5	-0.03
UK2	22	0.03	0.03	-0.18	173	0.05	0.17	0.27	173	11.17	15.41	0.08	174	10.63	1.27	0.06	123	615.3	108.2	0.00
UK3	-	-	-	-	205	0.07	0.17	0.12	166	11.93	22.69	0.77	209	11.71	2.09	0.10	159	724.3	132.3	-0.03
UK4	-	-	-	-	127	0.13	0.26	-0.41	172	4.70	3.94	0.24	127	9.38	2.06	0.07	42	690.8	96.36	-0.01
UK5	-	-	-	-	50	0.02	0.01	0.04	-	-	-	-	50	9.57	0.91	-0.03	54	665.8	49.59	0.04
UK6	21	0.10	0.02	0.24	210	0.13	0.09	-0.08	129	7.11	3.53	0.00	178	14.44	1.50	0.00	114	1770	429.5	-0.12
UK7	-	-	-	-	89	0.46	0.12	-0.10	5	5.00	2.12	0.32	54	11.27	1.58	-0.03	-	-	-	-
UK8	-	-	-	-	189	0.04	0.02	-0.21	142	9.52	12.18	0.55	152	10.64	1.55	0.13	138	570.8	110.4	0.05
UK9	-	-	-	-	210	0.43	0.35	-0.04	168	18.64	27.97	0.33	139	8.47	2.32	0.04	166	735.5	89.29	-0.01
UK10	-	-	-	-	71	0.68	0.56	-0.36	-	-	-	-	104	13.99	6.71	0.27	49	1088	248.9	-0.07
UK11	206	0.03	0.02	0.09	207	0.02	0.01	0.00	165	5.55	11.62	0.21	184	10.30	2.40	0.27	158	670.7	64.62	-0.03
UK12	-	-	-	-	176	0.36	0.25	-0.42	142	10.19	22.93	0.34	152	12.09	2.97	0.01	126	970.6	184.2	-0.12
UK13	-	-	-	-	164	0.27	0.31	-0.41	-	-	-	-	110	4.37	3.67	0.58	122	764.5	141.9	-0.07
UK14	-	-	-	-	79	0.02	0.01	0.06	-	-	-	-	79	6.95	2.25	0.27	79	731.1	282.9	0.03
UK15	-	-	-	-	140	0.20	0.13	-0.34	64	20.74	51.07	0.44	88	5.48	2.70	0.34	156	758.6	117.3	-0.05
UK16	46	0.21	0.17	0.28	224	0.10	0.08	0.00	-	-	-	-	164	5.71	3.86	0.50	155	782.1	78.08	-0.05
UK17	-	-	-	-	172	0.03	0.01	0.08	167	6.13	8.14	0.06	142	12.48	0.91	0.10	124	751.5	62.50	-0.01
UK18	-	-	-	-	90	0.66	0.46	-0.63	-	-	-	-	63	9.67	2.25	0.07	44	895.3	84.03	-0.01
UK19	-	-	-	-	118	0.38	0.18	-0.38	-	-	-	-	82	14.01	0.66	0.05	93	747.0	29.85	0.06
UK20	-	-	-	-	141	0.03	0.01	0.14	169	7.55	3.87	0.42	178	11.38	0.65	0.07	94	691.2	98.08	0.00
UK21	-	-	-	-	182	2.02	1.70	-0.20	115	19.70	18.07	-0.09	146	16.06	3.37	0.04	131	1332	324.0	-0.14
UK22	217	0.06	0.03	0.53	187	0.03	0.01	0.06	331	6.82	5.13	1.16	151	3.37	0.72	0.40	225	814.2	50.73	-0.05
UK23	927	0.62	1.19	0.29	1015	0.27	0.13	-0.01	926	58.56	144.2	0.90	978	10.83	3.05	0.03	67	1043	122.6	-0.12

UK24	-	-	-	-	169	0.27	0.13	-0.34	168	9.30	11.18	0.73	140	7.93	2.04	0.14	155	817.4	55.76	-0.02
UK25	-	-	-	-	101	0.12	0.12	-0.02	-	-	-	-	65	6.87	4.65	0.41	52	851.0	73.76	-0.06
UK26	-	-	-	-	134	0.07	0.04	0.08	-	-	-	-	98	5.90	3.76	0.37	113	840.7	70.57	-0.04
UK27	-	-	-	-	142	1.30	1.32	-0.68	-	-	-	-	103	10.82	6.20	0.05	100	936.8	188.9	-0.10
UK28	-	-	-	-	188	0.55	0.27	-0.36	141	14.75	35.26	1.19	152	10.61	1.74	-0.11	151	986.9	150.4	-0.22
UK29	-	-	-	-	176	0.51	0.35	-0.38	72	13.40	25.19	0.55	140	7.40	3.96	0.07	82	832.7	194.6	-0.02
UK30	-	-	-	-	138	0.56	0.35	-0.55	123	13.67	13.64	0.18	102	7.10	3.74	0.29	44	819.1	125.4	-0.02
UK31	-	-	-	-	122	0.08	0.16	0.06	6	13.74	5.89	0.62	85	5.63	2.19	0.14	18	734.8	130.8	-0.09
UK32	-	-	-	-	209	0.07	0.05	0.47	168	6.80	15.78	0.29	173	9.94	2.10	0.11	115	743.4	37.60	-0.03
UK33	-	-	-	-	-	-	-	-	-	-	-	-	106	8.70	1.60	0.22	18	668.1	26.04	0.03
UK34	20	0.03	0.01	-0.01	92	0.05	0.05	0.26	20	3.64	0.86	0.04	92	7.94	0.56	0.02	17	606.8	23.77	0.03
UK35	-	-	-	-	114	0.02	0.01	0.00	160	5.19	5.46	-0.03	85	8.87	1.19	0.07	28	543.9	93.23	-0.02
UK36	-	-	-	-	134	0.23	0.33	0.16	-	-	-	-	107	7.22	3.77	0.36	-	-	-	-
UK37	-	-	-	-	167	0.20	0.15	-0.42	159	11.54	18.13	0.40	202	6.52	3.21	0.25	89	777.1	223.3	-0.17
UK38	-	-	-	-	161	0.09	0.10	0.29	175	11.15	12.79	0.69	161	8.55	1.71	-0.02	68	735.9	107.6	-0.11
UK39	-	-	-	-	84	0.09	0.10	-0.02	60	12.58	12.96	0.17	84	7.90	1.93	0.18	80	586.1	53.22	0.02
UK40	-	-	-	-	-	-	-	-	-	-	-	-	104	9.04	1.96	-0.19	48	813.9	149.4	-0.18
UK41	-	-	-	-	144	0.39	0.21	-0.35	6	8.91	8.83	0.88	106	10.15	1.59	-0.05	51	645.4	120.6	-0.21
UK42	-	-	-	-	151	0.01	0.01	0.32	141	3.84	0.45	0.15	152	0.47	0.31	0.03	95	154.4	47.60	-0.24

Supplementary Table ST2 Relative error (mean ***μ***, standard deviation ***δ***, minimum ***Min*** and maximum ***Max***) **in mean concentrations** estimated from resampled water quality datasets based on 10,000 Monte Carlo iterations

Determinand	**Sampling**	**HF1**				**HF2**			
		μ	***δ***	***Min***	***Max***	***μ***	***δ***	***Min***	***Max***
TP (mgl^{-1})	*Daily*	0.2	3.7	-16.5	12.1	0.7	3.2	-9.6	10.4
	Weekly	0.3	14.7	-73.7	35.7	0.1	10.1	-63.5	22.2
	Fortnightly	0.3	23.0	-113.7	47.4	-0.1	16.7	-116.2	28.2
	Monthly	1.9	34.4	-254.8	59.7	3.2	26.1	-288.1	42.0
TRP (mgl^{-1})	*Daily*	6.6	1.6	-0.5	11.4	0.5	2.1	-7.7	8.6
	Weekly	6.2	5.5	-25.9	21.4	2.0	6.3	-21.1	25.0
	Fortnightly	6.2	8.4	-50.0	30.3	-0.3	10.4	-42.3	34.5
	Monthly	6.6	13.0	-99.4	45.9	5.9	19.7	-55.3	74.8
TURB (NTU)	*Daily*	4.6	4.2	-19.3	17.1	1.1	5.9	-28.6	15.7
	Weekly	3.2	14.3	-87.0	34.0	-4.7	19.3	-156.2	30.6
	Fortnightly	3.7	20.4	-185.7	39.1	-1.5	29.6	-250.3	44.0
	Monthly	4.2	30.4	-304.8	47.3	0.7	45.1	-440.9	54.6
NO_3-N (mgl^{-1})	*Daily*	-5.4	0.3	-6.5	-4.4	-0.1	2.4	-8.2	7.5
	Weekly	-5.5	1.3	-11.3	-0.8	-4.7	14.5	-58.2	22.4
	Fortnightly	-5.6	2.0	-13.7	2.7	-1.6	22.3	-85.9	36.9
	Monthly	-5.7	3.2	-21.4	11.1	0.6	34.2	-304.6	48.7
COND/DOC ($\mu Sm^{-1}/mgl^{-1}$)	*Daily*	-2.3	0.2	-2.9	-1.6	0.3	0.9	-2.8	4.2
	Weekly	-2.2	0.8	-6.0	0.9	-2.2	4.6	-20.3	13.8
	Fortnightly	-2.3	1.3	-7.5	2.7	0.5	8.5	-31.9	27.3
	Monthly	-2.4	2.0	-11.1	7.0	0.4	12.5	-51.5	32.2

Supplementary Table ST3 Relative error (mean ***μ***, standard deviation ***δ***, minimum ***Min*** and maximum ***Max***) **in standard deviation of the concentrations** estimated from resampled water quality datasets based on 10,000 Monte Carlo iterations

Determinand	**Sampling**	**HF1**				**HF2**			
		μ	***δ***	***Min***	***Max***	***μ***	***δ***	***Min***	***Max***
TP (mgl^{-1})	*Daily*	0.9	12.0	-50.0	27.5	3.6	24.9	-63.3	47.2
	Weekly	7.0	37.0	-181.4	74.6	17.8	46.5	-208.5	76.8
	Fortnightly	13.8	51.5	-275.9	82.3	21.9	57.8	-357.1	91.5
	Monthly	23.9	63.0	-386.0	90.5	28.0	72.1	-649.7	100.0
TRP (mgl^{-1})	*Daily*	4.5	13.9	-71.4	26.2	-0.3	5.1	-18.3	17.9
	Weekly	7.4	28.9	-216.2	43.7	5.7	18.0	-54.3	66.7
	Fortnightly	9.4	35.8	-296.4	53.4	3.8	28.5	-95.6	86.6
	Monthly	13.8	42.4	-466.6	67.7	7.2	53.4	-217.0	100.0
TURB (NTU)	*Daily*	-6.0	21.7	-134.1	46.6	3.9	23.9	-133.7	46.8
	Weekly	1.6	52.9	-341.2	74.9	12.1	46.4	-373.1	71.9
	Fortnightly	9.2	62.2	-573.9	81.1	18.5	58.0	-521.6	82.3
	Monthly	20.4	75.6	-771.7	86.0	27.1	69.3	-815.3	90.9
NO_3-N (mgl^{-1})	*Daily*	-1.0	2.9	-12.9	8.5	0.0	7.1	-23.4	18.0
	Weekly	-0.8	10.3	-54.2	26.0	6.2	31.5	-90.0	42.6
	Fortnightly	-0.5	15.1	-94.1	36.3	7.2	42.4	-156.6	52.7
	Monthly	1.0	22.0	-147.2	48.6	10.3	53.4	-299.4	66.6
COND/DOC ($\mu Sm^{-1}/mgl^{-1}$)	*Daily*	7.0	3.0	-2.6	16.3	0.3	2.7	-9.3	9.0
	Weekly	8.0	12.5	-47.3	38.4	-1.8	10.4	-40.9	35.6
	Fortnightly	9.0	18.3	-83.5	50.6	0.0	19.3	-75.5	61.7
	Monthly	11.2	26.2	-138.7	69.1	-2.8	29.7	-127.0	72.8

Supplementary Table ST4 Relative error (mean ***μ***, standard deviation ***δ***, minimum ***Min*** and maximum ***Max***) **in maximum concentrations** estimated from resampled water quality datasets based on 10,000 Monte Carlo iterations. Minimum error is 0 in all cases as at least one of the resampled datasets contains the absolute maximum value

Determinand	**Sampling**	**HF1**				**HF2**			
		μ	***δ***	***Min***	***Max***	***μ***	***δ***	***Min***	***Max***
TP (mgl^{-1})	*Daily*	39.2	17.6	0.0	61.5	37.3	20.9	0.0	70.7
	Weekly	63.5	17.1	0.0	94.5	64.6	15.0	0.0	80.7
	Fortnightly	74.1	17.7	0.0	96.6	70.2	12.4	0.0	82.9
	Monthly	83.0	15.3	0.0	97.7	75.6	10.1	0.0	88.6
TRP (mgl^{-1})	*Daily*	56.0	20.2	0.0	83.7	2.7	2.8	0.0	11.8
	Weekly	78.0	13.3	0.0	91.7	19.7	12.9	0.0	50.0
	Fortnightly	82.6	11.0	0.0	93.8	27.7	13.1	0.0	55.9
	Monthly	86.8	8.4	0.0	95.7	40.6	17.0	0.0	85.3
TURB (NTU)	*Daily*	61.1	14.7	0.0	89.6	62.5	15.0	0.0	87.4
	Weekly	80.6	13.1	0.0	97.6	81.6	11.1	0.0	94.8
	Fortnightly	86.3	10.8	0.0	98.3	86.5	9.5	0.0	96.5
	Monthly	91.1	9.3	0.0	98.8	90.6	7.7	0.0	97.2
NO_3-N (mgl^{-1})	*Daily*	38.3	13.6	0.0	52.4	13.0	10.8	0.0	39.8
	Weekly	49.8	7.5	0.0	58.3	59.2	21.7	0.0	79.5
	Fortnightly	52.3	6.4	0.0	60.1	67.9	18.7	0.0	86.8
	Monthly	54.7	5.5	0.0	62.9	76.1	14.9	0.0	90.0
COND/DOC ($\mu Sm^{-1}/mgl^{-1}$)	*Daily*	19.2	12.8	0.0	54.1	14.0	8.5	0.0	29.9
	Weekly	45.6	13.8	0.0	61.7	27.5	7.8	0.0	49.2
	Fortnightly	51.7	11.9	0.0	62.5	33.5	9.3	0.0	57.7
	Monthly	56.2	9.8	0.0	63.5	40.1	10.5	0.0	66.0

Supplementary Table ST5 Relative error (mean ***μ***, standard deviation ***δ***, minimum ***Min*** and maximum ***Max***) **in 95th percentile** of the concentrations estimated from resampled water quality datasets based on 10,000 Monte Carlo iterations

Determinand	**Sampling**	**HF1**				**HF2**			
		μ	***δ***	***Min***	***Max***	***μ***	***δ***	***Min***	***Max***
TP (mgl^{-1})	*Daily*	0.0	6.0	-30.8	18.7	-2.7	6.3	-47.5	16.1
	Weekly	-3.8	24.7	-272.3	44.9	-14.5	44.9	-221.0	35.8
	Fortnightly	-10.8	47.9	-461.0	55.3	0.6	41.4	-233.1	42.9
	Monthly	-35.6	94.9	-885.1	72.1	18.8	33.7	-233.1	61.9
TRP (mgl^{-1})	*Daily*	7.9	2.7	-5.6	18.0	-1.8	8.2	-21.7	16.6
	Weekly	6.0	10.1	-49.5	35.7	1.1	14.6	-25.2	37.0
	Fortnightly	5.8	15.0	-132.0	43.8	9.0	16.5	-25.9	44.4
	Monthly	4.5	26.0	-301.8	53.9	25.2	21.5	-25.9	81.5
TURB (NTU)	*Daily*	-0.6	5.9	-34.4	15.8	1.1	11.1	-76.8	29.2
	Weekly	-5.9	22.6	-203.5	35.4	-22.0	52.2	-533.7	54.4
	Fortnightly	-11.8	39.1	-428.9	46.8	-18.6	81.8	-765.3	68.4
	Monthly	-27.3	75.6	-1375.8	61.4	15.7	69.5	-799.7	74.5
NO_3-N (mgl^{-1})	*Daily*	-2.9	0.5	-5.2	-0.9	0.8	4.4	-12.6	15.6
	Weekly	-2.9	1.9	-16.4	3.0	-18.0	37.2	-141.9	31.0
	Fortnightly	-3.1	3.2	-30.6	5.8	-21.8	68.9	-272.5	49.0
	Monthly	-3.6	5.9	-64.0	10.6	7.5	57.7	-286.6	61.4
COND/DOC ($\mu Sm^{-1}/mgl^{-1}$)	*Daily*	-0.9	0.3	-2.3	0.0	0.3	1.8	-4.7	7.3
	Weekly	-0.9	1.1	-9.1	1.9	0.7	7.7	-27.5	26.6
	Fortnightly	-1.1	1.8	-16.4	3.2	3.8	13.2	-44.2	39.0
	Monthly	-1.7	3.6	-38.0	4.1	12.7	15.4	-45.8	50.5

Supplementary Table ST6 Relative error (mean ***μ***, standard deviation ***δ***, minimum ***Min*** and maximum ***Max***) **in load** estimated from resampled water quality datasets based on 10,000 Monte Carlo iterations

Determinand	**Sampling**	**HF1**				**HF2**			
		μ	***δ***	***Min***	***Max***	***μ***	***δ***	***Min***	***Max***
TP (mgl^{-1})	*Daily*	1.3	18.4	-62.9	43.5	9.4	34.4	-167.5	51.3
	Weekly	10.1	41.2	-196.0	76.1	26.1	30.6	-236.0	64.0
	Fortnightly	17.0	48.0	-266.7	80.7	29.1	30.0	-236.0	64.0
	Monthly	25.7	53.1	-464.4	88.9	32.6	28.8	-236.0	64.0
TRP (mgl^{-1})	*Daily*	-2.3	12.0	-46.3	26.8	-3.1	14.1	-86.8	68.0
	Weekly	3.4	28.9	-135.4	48.2	-11.9	28.6	-153.0	91.2
	Fortnightly	7.9	33.6	-162.6	55.6	-19.0	38.7	-153.0	92.6
	Monthly	14.7	37.0	-196.8	69.5	-17.0	45.6	-153.0	92.6
TURB (NTU)	*Daily*	-4.3	22.7	-121.9	51.8	12.6	44.5	-206.7	72.8
	Weekly	2.4	66.6	-556.1	78.3	40.6	44.9	-307.3	96.8
	Fortnightly	9.8	80.8	-1051.6	83.4	52.4	41.7	-509.3	96.2
	Monthly	22.6	98.0	-1642.3	87.4	60.1	38.8	-313.9	97.3
NO_3-N (mgl^{-1})	*Daily*	-4.1	3.1	-14.7	9.1	0.0	17.5	-131.8	47.3
	Weekly	-4.7	7.9	-40.0	38.8	7.3	38.3	-359.5	96.6
	Fortnightly	-5.0	10.0	-45.1	55.6	17.6	51.9	-414.7	117.3
	Monthly	-5.3	11.7	-66.4	64.5	29.4	56.8	-414.7	117.3
COND/DOC ($\mu Sm^{-1}/mgl^{-1}$)	*Daily*	-1.0	4.1	-13.3	12.1	3.2	10.4	-39.9	40.9
	Weekly	-4.0	11.3	-28.4	33.7	14.2	19.4	-62.1	81.3
	Fortnightly	-6.6	13.9	-34.7	42.4	23.9	23.8	-63.5	81.3
	Monthly	-10.0	15.9	-41.7	50.3	29.3	25.1	-63.5	81.3

Supplementary Table ST7 *c-q* slope calculation (mean ***μ***, standard deviation ***δ***, minimum ***Min*** and maximum ***Max***) from resampled water quality datasets based on 10,000 Monte Carlo iterations

Determinand	**Sampling**	**HF1**				**HF2**			
		μ	***δ***	***Min***	***Max***	***μ***	***δ***	***Min***	***Max***
TP (mgl^{-1})	*HF*	0.36				0.09			
	LF	0.29				-0.09			
	Daily	0.36	0.01	0.30	0.40	0.17	0.05	-0.24	0.42
	Weekly	0.35	0.05	0.15	0.55	0.18	0.32	-0.17	0.78
	Fortnightly	0.36	0.07	0.17	0.69	0.12	0.33	-0.25	0.81
	Monthly	0.42	0.10	0.19	1.03	0.20	0.34	-0.14	0.58
TRP (mgl^{-1})	*HF*	0.24				-0.13			
	LF	0.17				-0.20			
	Daily	0.26	0.01	0.22	0.29	-0.20	0.08	-0.81	-0.08
	Weekly	0.26	0.03	0.13	0.41	-0.25	0.48	-0.42	0.52
	Fortnightly	0.27	0.05	0.13	0.52	-0.27	0.76	-0.16	0.93
	Monthly	0.31	0.07	0.16	0.61	1.99	0.95	-0.92	1.63
TURB (NTU)	*HF*	0.32				0.27			
	LF	0.35				0.36			
	Daily	0.35	0.01	0.31	0.41	0.27	0.04	0.09	0.43
	Weekly	0.35	0.05	0.19	0.54	0.31	0.12	-0.24	0.94
	Fortnightly	0.35	0.07	0.13	0.61	0.33	0.15	-0.64	0.61
	Monthly	0.36	0.10	0.14	0.81	0.30	0.17	-0.75	0.58
NO_3-N (mgl^{-1})	*HF*	-0.04				0.42			
	LF	0.01				0.30			
	Daily	-0.04	0.01	-0.08	-0.02	0.42	0.05	0.27	0.74
	Weekly	-0.07	0.03	-0.26	0.05	0.49	0.16	0.08	0.49
	Fortnightly	-0.10	0.06	-0.46	0.09	0.55	0.31	0.02	0.75
	Monthly	-0.11	0.12	-0.85	0.32	0.54	0.28	0.12	1.37
COND/DOC ($\mu Sm^{-1}/mgl^{-1}$)	*HF*	-0.07				0.11			
	LF	-0.05				0.06			
	Daily	-0.06	0.00	-0.07	-0.04	0.11	0.02	0.05	0.20
	Weekly	-0.06	0.01	-0.10	-0.02	0.15	0.08	-0.08	1.07
	Fortnightly	-0.06	0.02	-0.12	-0.02	0.17	0.29	-0.40	0.37
	Monthly	-0.07	0.02	-0.19	0.03	0.20	0.24	-0.02	0.63

Supplementary Table ST8 Comparison between single linear (c-$q_{Q<>}$) and two linear c-q slopes (c-$q_{Q<}$ for flows lower than the threshold value Q and c-$q_{Q>}$ for flows higher than the threshold value Q) for time series showing step changes in the c-q relationship. Slopes which are not significant at 0.05 level are marked with ~~strikethrough~~. Flow-proportional datasets are marked with ^{fp}

Dataset	c-$q_{Q<>}$	c-$q_{Q<}$	c-$q_{Q>}$	Q (m^3s^{-1})	Q percentile
TP	p=0.03				
SE1	0.11	-0.10	0.53	0.30	44
SE6	0.06	-0.16	0.28	0.10	53
SE9	-0.06	-0.29	0.54	0.31	71
NO5^{fp}	0.74	0.75	1.00	0.05	91
NO6^{fp}	0.21	-0.05	0.34	0.32	53
UK23	0.29	-0.07	0.22	0.25	40
RP	p=0.07				
SE9	-0.16	-0.29	0.31	0.27	71
SE10	0.21	-0.02	0.46	0.10	47
UK7	-0.10	-0.43	~~0.40~~	0.63	90
UK13	-0.41	-0.66	0.21	0.30	82
UK36	0.26	~~-0.16~~	~~0.50~~	0.29	64
SS	p=0.02				
NO3^{fp}	0.56	0.36	0.73	0.06	77
NO6^{fp}	0.54	0.22	0.55	0.30	53
NO9^{fp}	0.53	0.36	0.58	0.10	80
UK23	0.90	0.41	0.59	0.31	40
NO_3-N	p=0.17				
HF2	0.42	0.10	0.28	0.01	62
SE2	0.62	0.44	0.37	0.28	70
UK16	0.50	0.84	0.00	0.03	22
DOC	-				
HF2	0.11	0.04	0.25	0.01	62
COND	p=0.10				
HF1	-0.07	-0.06	-0.26	10.0	98
SE10	-0.18	-0.04	-0.28	0.10	47

Supplementary Table ST9 Linear trends for flow and water quality time series in the study catchments. An annual change in flow and concentrations is given and expressed in percentage terms (annual change divided by the mean flow/concentration). Annual trends which are not significant at 0.05 level are marked with ~~strikethrough~~. Flow-proportional datasets are marked with ^{fp}

Dataset	Q	TP	RP	SS $_{LF}$ TURB$_{HF}$	NO_3-N	DOC	COND
HF1	-9.69	~~3.18~~	2.78	8.68	-6.72	-	-2.13
LF1	0.78	0.56	-0.72	1.73	~~-0.28~~	-2.26	~~0.13~~
HF2	8.30	-2.20	-5.18	4.35	4.86	1.85	-
LF2	-	~~-2.24~~	-	~~5.31~~	-1.26	-	~~0.20~~
SE1	~~0.53~~	~~-0.57~~	-3.61	~~2.67~~	~~0.45~~	1.04	-0.45
SE2	1.17	-3.14	~~0.37~~	~~-1.60~~	-0.95	2.57	~~-0.11~~
SE3	0.78	0.56	-0.72	1.73	~~-0.28~~	-2.26	~~0.13~~
SE4	1.02	~~0.94~~	2.72	4.61	-2.95	2.54	-1.46
SE5	-1.27	5.03	2.63	~~1.05~~	-3.56	2.29	0.99
SE6	0.77	-4.07	-6.76	-2.34	-2.35	-2.38	~~0.08~~
SE7	1.70	-5.00	-5.97	-4.00	-1.22	-2.32	-0.60
SE8	0.52	~~-0.83~~	~~1.02~~	~~0.90~~	-3.20	0.87	-0.89
SE9	0.64	-1.49	-4.24	5.15	-1.42	-10.05	-0.39
SE10	~~0.00~~	-1.62	-12.79	4.65	-3.18	-0.74	1.07
SE1^{fp}	~~0.53~~	3.11	4.83	~~-0.37~~	2.44	-2.54	~~-0.66~~
SE2^{fp}	1.17	~~3.13~~	~~0.23~~	8.50	~~0.42~~	-3.35	~~1.18~~
SE3^{fp}	0.78	-4.06	~~-2.96~~	-10.67	~~-2.16~~	-2.48	2.48
SE4^{fp}	1.02	~~0.53~~	4.97	-7.23	1.11	-5.53	-2.31
SE5^{fp}	-1.27	9.46	11.58	5.62	~~-1.93~~	-4.96	~~1.14~~
SE6^{fp}	0.77	4.24	3.84	~~0.79~~	0.76	-4.78	~~1.29~~
SE7^{fp}	1.70	10.50	16.72	~~1.29~~	1.60	-2.18	~~0.22~~
SE8^{fp}	0.52	~~2.17~~	~~-0.76~~	~~2.49~~	0.97	-3.73	~~0.65~~
SE9^{fp}	0.64	~~1.21~~	3.48	~~-3.27~~	~~-2.50~~	-3.78	~~1.84~~
SE10^{fp}	0.00	-4.66	~~0.71~~	-17.44	-8.00	-2.77	3.70
NO1^{fp}	~~0.13~~	~~-0.22~~	~~0.29~~	-4.55	-	-	-
NO2^{fp}	~~-1.94~~	7.17	3.22	~~0.49~~	~~-1.03~~	-	-
NO3^{fp}	~~1.04~~	2.24	~~0.80~~	3.74	-0.98	-	-
NO4^{fp}	~~4.74~~	~~-2.44~~	~~5.75~~	-17.88	-7.79	-	-
NO5^{fp}	1.80	-3.65	1.11	-6.78	~~-0.35~~	-	-
NO6^{fp}	~~0.13~~	1.92	-10.57	2.31	1.12	-	-
NO7^{fp}	~~0.17~~	-1.81	-15.92	~~1.89~~	-0.63	-	-
NO8^{fp}	~~0.72~~	~~0.57~~	2.19	~~-2.01~~	~~-0.33~~	-	-
NO9^{fp}	-1.66	~~-0.67~~	-1.64	~~1.24~~	~~-0.65~~	-	-
NO10^{fp}	-1.87	~~-2.27~~	-5.23	~~1.23~~	-1.49	-	-
UK1	1.40	-	~~-1.15~~	~~-2.75~~	-3.77	-	~~2.19~~
UK2	0.06	~~-3.25~~	~~3.99~~	6.77	0.51	-	0.53
UK3	1.56	-	-12.93	-7.14	-0.81	-	~~0.13~~
UK4	1.28	-	-9.38	~~0.52~~	1.15	-	~~0.86~~
UK5	0.53	-	-16.84	-	~~-0.56~~	-	-2.12
UK6	-0.06	~~-6.77~~	-8.38	-3.22	~~0.14~~	-	-3.76
UK7	0.17	-	-4.25	-	~~0.09~~	-	-
UK8	-0.09	-	~~-1.48~~	~~0.11~~	-0.73	-	~~-0.48~~
UK9	0.68	-	~~-0.19~~	~~-1.28~~	~~-0.58~~	-	~~-0.33~~

UK10	-0.65	-	~~-2.28~~	-	~~-1.94~~	-	1.76
UK11	-0.72	~~0.10~~	~~-0.82~~	~~-1.59~~	-1.55	-	~~0.17~~
UK12	-1.26	-	~~-0.02~~	~~-3.50~~	-2.03	-	0.78
UK13	0.82	-	-4.00	-	~~1.40~~	-	~~0.19~~
UK14	0.40	-	-14.34	-	~~0.84~~	-	~~-2.08~~
UK15	1.56	-	3.65	~~28.88~~	~~-4.38~~	-	~~0.03~~
UK16	~~-0.05~~	~~-19.39~~	-3.90	-	~~-1.49~~	-	~~0.19~~
UK17	-0.11	-	~~0.18~~	~~2.91~~	~~-0.19~~	-	0.28
UK18	0.19	-	~~1.81~~	-	2.53	-	~~0.13~~
UK19	-0.26	-	~~-1.25~~	-	-0.36	-	~~-0.08~~
UK20	0.31	-	~~-0.04~~	~~-0.55~~	0.21	-	~~0.32~~
UK21	1.00	-	-13.58	-9.29	-1.20	-	~~-0.34~~
UK22	0.50	-3.35	~~-0.87~~	-3.14	-3.33	-	~~0.07~~
UK23	0.58	-7.00	~~-0.35~~	-11.45	-1.83	-	~~0.11~~
UK24	0.42	-	-5.50	~~-3.32~~	-1.24	-	-0.21
UK25	0.39	-	~~4.29~~	-	~~-3.08~~	-	~~0.03~~
UK26	0.74	-	-1.58	-	~~-0.37~~	-	~~0.02~~
UK27	~~0.06~~	-	~~-1.69~~	-	~~-1.81~~	-	1.08
UK28	0.64	-	-1.65	~~-2.22~~	~~-0.03~~	-	~~0.34~~
UK29	~~0.25~~	-	~~-0.44~~	~~21.83~~	~~-1.02~~	-	~~0.25~~
UK30	~~-0.10~~	-	~~-1.09~~	~~2.52~~	~~-1.41~~	-	~~1.21~~
UK31	0.74	-	~~-0.22~~	~~-149.00~~	~~-1.17~~	-	~~-1.54~~
UK32	-0.52	-	-4.56	~~-0.30~~	~~0.40~~	-	~~0.11~~
UK33	0.56	-	-	-	~~0.87~~	-	-1.42
UK34	0.97	~~-3.53~~	~~-2.97~~	~~-12.09~~	~~0.21~~	-	~~-0.34~~
UK35	0.82	-	~~-1.55~~	4.90	-3.64	-	~~8.00~~
UK36	~~-0.20~~	-	~~0.91~~	-	~~-5.84~~	-	~~-2.98~~
UK37	~~0.10~~	-	~~-0.38~~	~~-4.78~~	-1.91	-	~~1.21~~
UK38	0.41	-	~~-1.42~~	-6.10	-1.38	-	~~-1.29~~
UK39	0.79	-	13.47	~~0.69~~	3.15	-	~~0.09~~
UK40	2.00	-	-	-	-1.28	-	~~0.65~~
UK41	0.20	-	9.32	-2.67	-4.33	-	~~-0.09~~
UK42	0.15	-	-2.09	~~7.92~~	-2.94	-	0.52

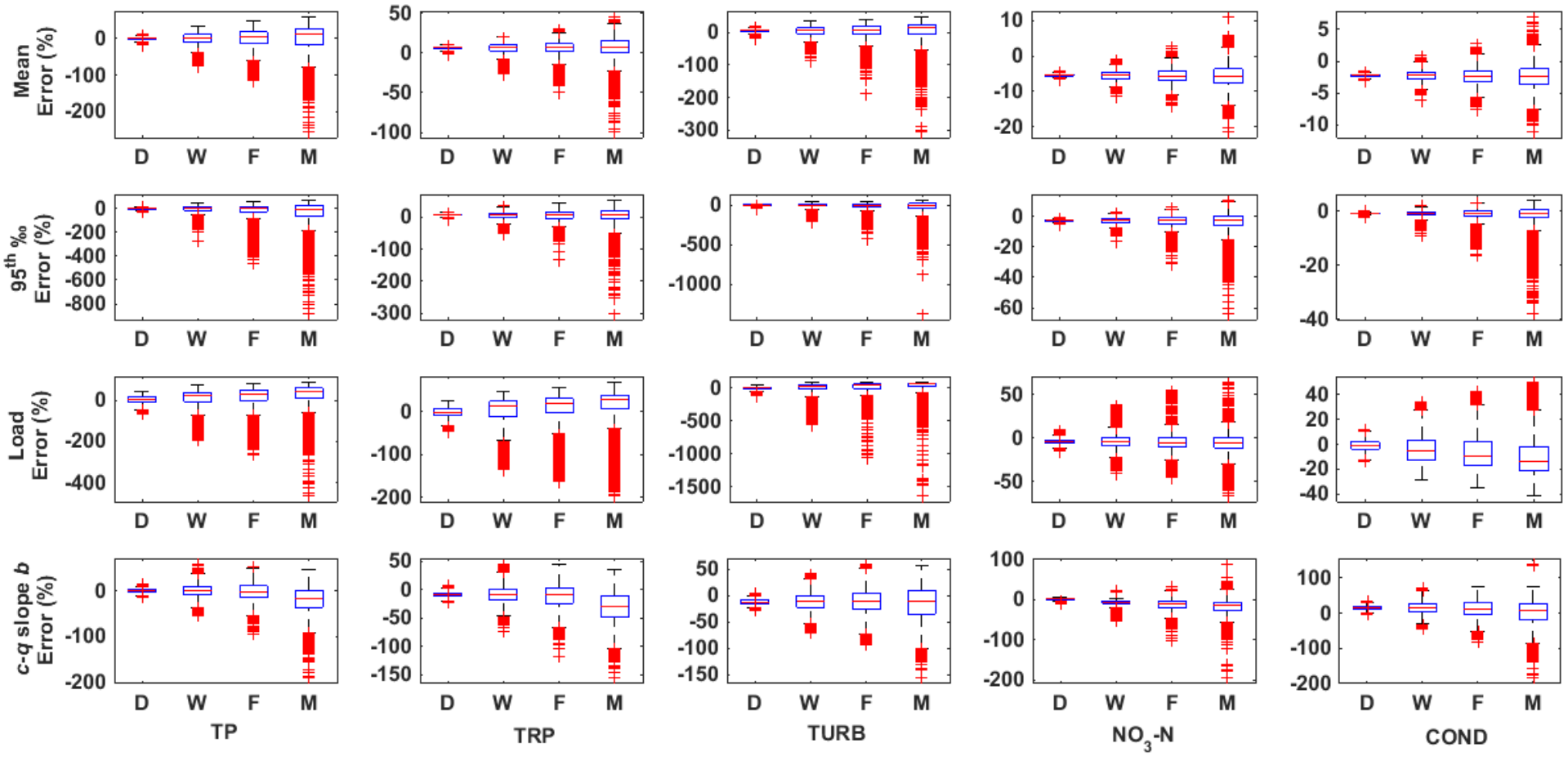

Supplementary Figure SF1 Relative errors in mean (top row), 95th percentile (second row), load estimation (third row) and *c-q* slope (bottom row) for **HF1** for TP, TRP, TURB, NO_3-N and COND. The central red mark is the median, the edges of the box are the 25th and 75th percentiles, the black whiskers extend to the most extreme data points and outliers are plotted as red crosses

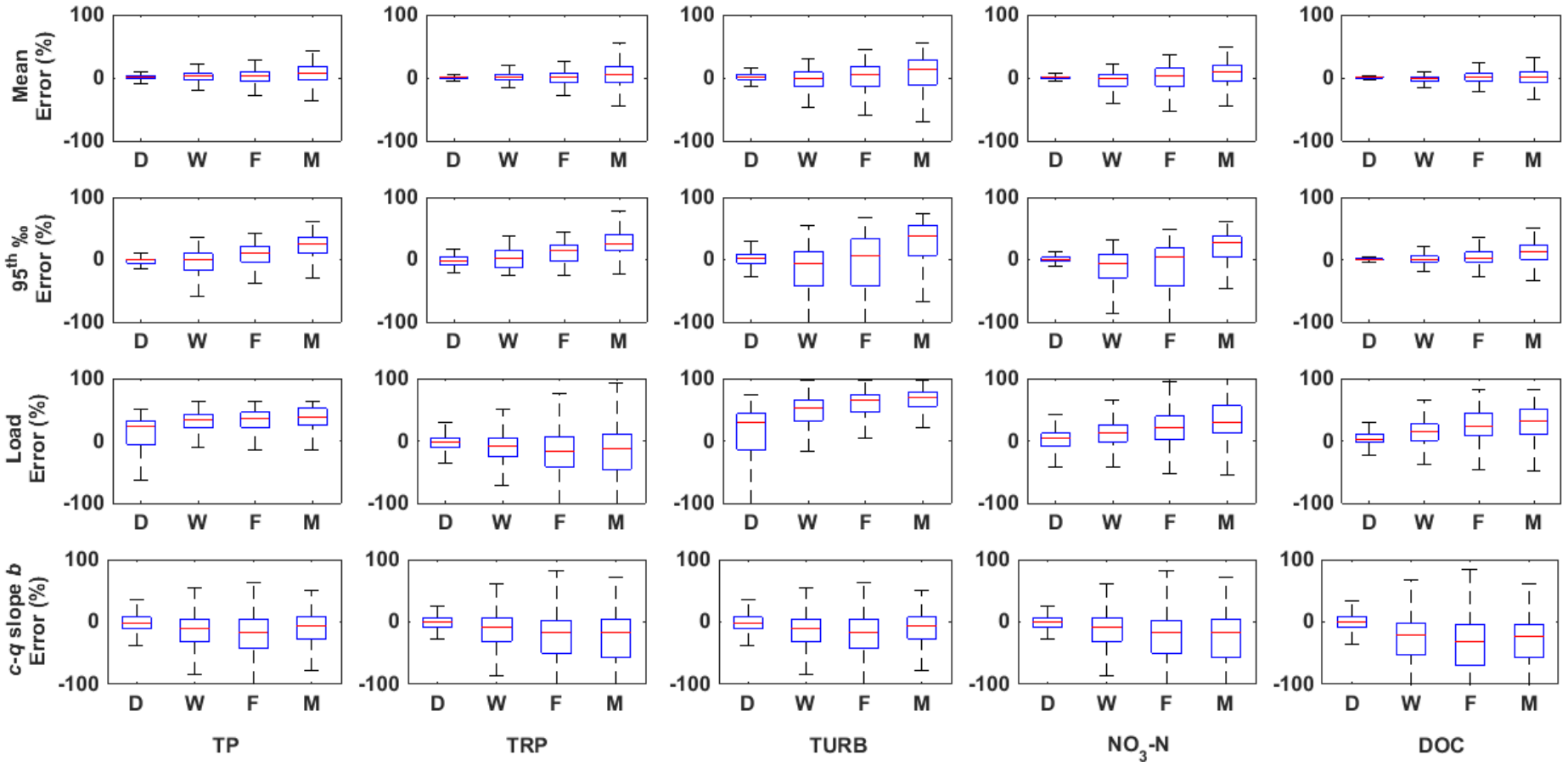

Supplementary Figure SF2 Relative errors in mean (top row), 95th percentile (second row), load estimation (third row) and *c*-*q* slope (bottom row) for **HF2** for TP, TRP, TURB, NO_3-N and COND. The central red mark is the median, the edges of the box are the 25th and 75th percentiles, the black whiskers extend to the most extreme data points. For better clarity the figure does not contain outliers (given in Supplementary Figure SF3)

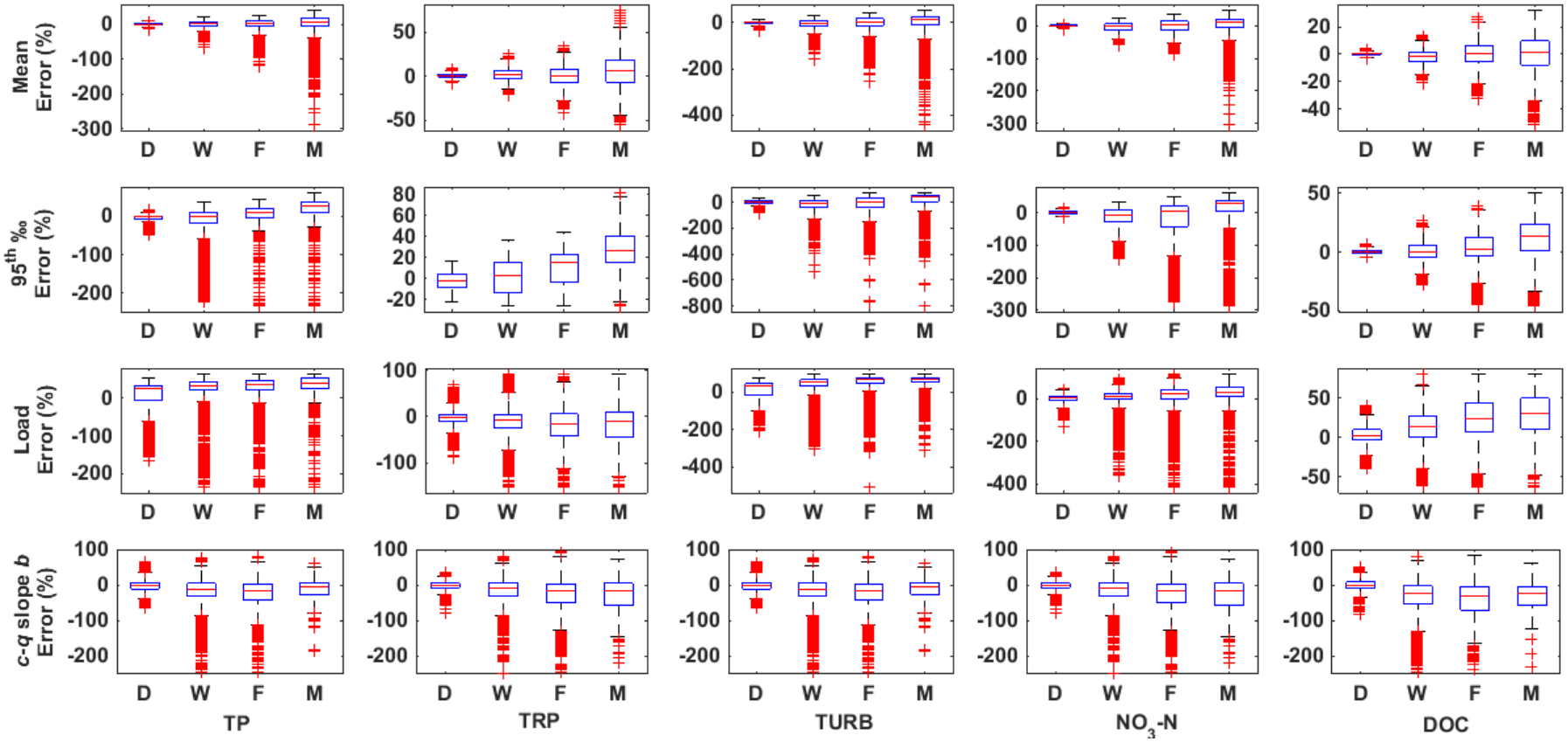

Supplementary Figure SF3 Relative errors in mean (top row), 95th percentile (second row), load estimation (third row) and *c-q* slope (bottom row) for **HF2** for TP, TRP, TURB, NO_3-N and COND. The central red mark is the median, the edges of the box are the 25th and 75th percentiles, the black whiskers extend to the most extreme data points and outliers are plotted as red crosses

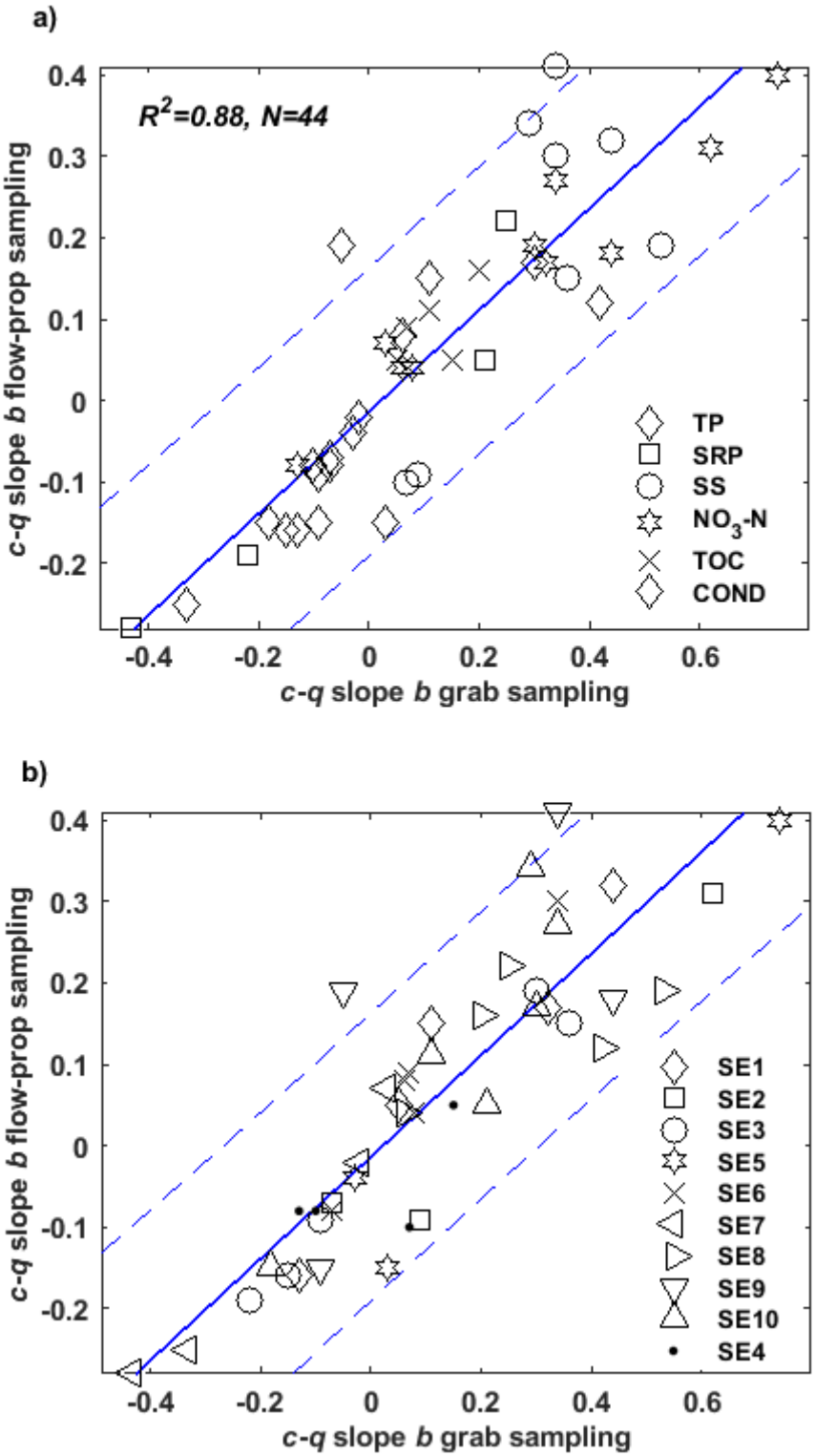

Supplementary Figure SF4 Relationship between *c-q* slope *b* calculated from the grab (horizontal axes) and flow-proportional sampling (vertical axes) for determinands (a) and catchments (b)

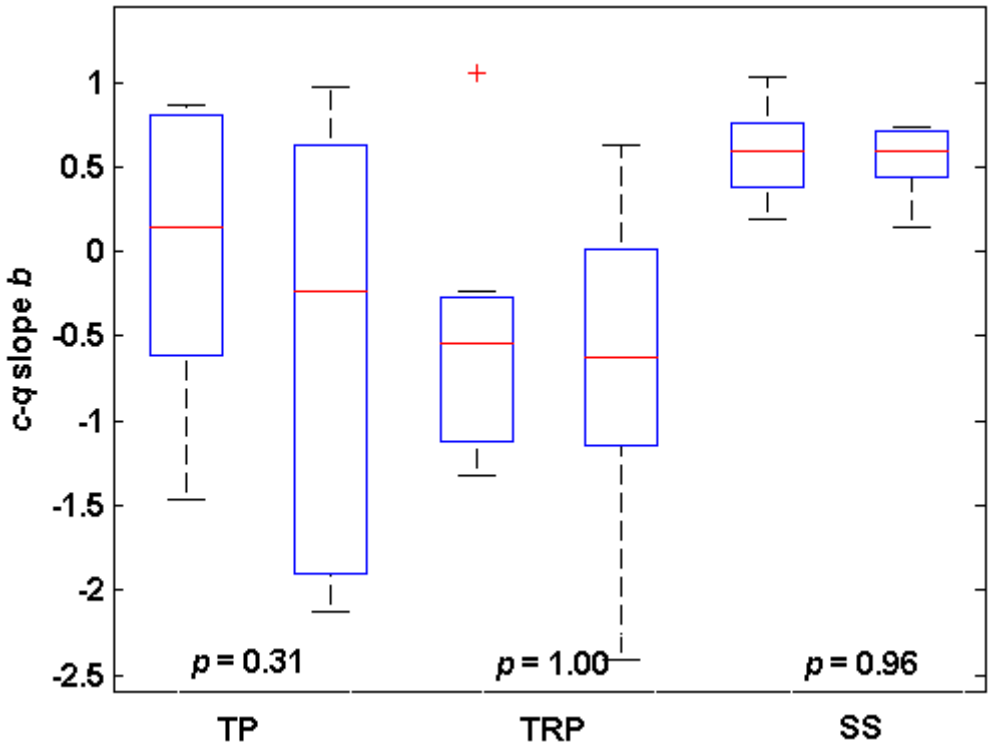

Supplementary Figure SF5 Analysis of variance (Kruskal-Wallis one-way ANOVA) for the *c*-*q* slopes *b* for annual linear trends >5%. For each determinand datasets showing >5% linear trends (as in Supplementary Table ST9), were divided into two sub-datasets and *c*-*q* slopes were calculated independently for each half. The central red mark is the mean, the edges of the box are the 25th and 75th percentiles, the black whiskers extend to the most extreme data points and outliers are plotted as red crosses

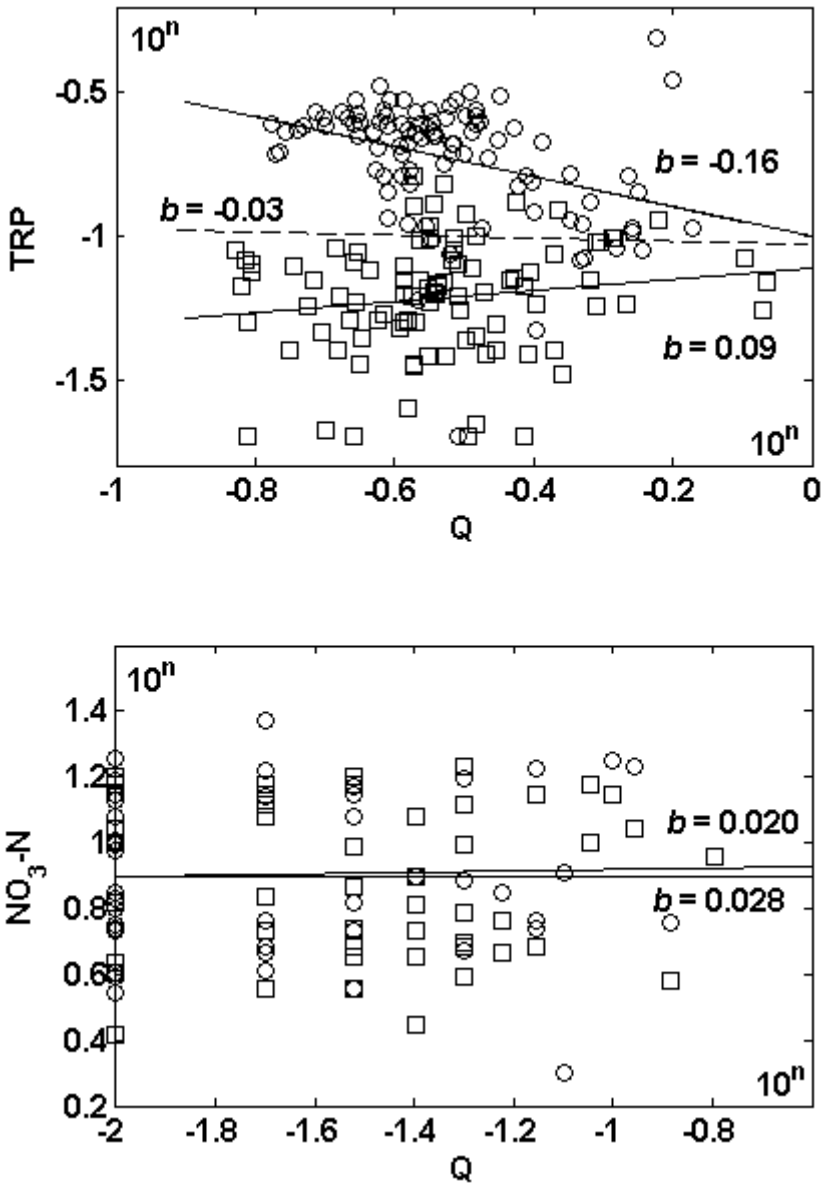

Supplementary Figure SF6 The effect of linear trends on the *c-q* slopes *b* for TRP and NO_3-N for the catchments UK6 (top figure) and NO4 (bottom figure). Both determinands for these catchments show significant annual linear trends of -8.38% and -7.79% respectively (Supplementary Table ST9). The time series were split in half (circles for the first half and squares for the second half) and *c-q* slopes were calculated independently for each half with the best fit line fitted. The dashed line indicates the best fit line fitted to the whole time series. All axes are in logarithmic scale